



HAL
open science

Linking multiple facets of biodiversity and ecosystem functions in a coastal reef habitat

Auriane Jones, Lionel Denis, Jérôme Fournier, Nicolas Desroy, Gwendoline Duong, Stanislas Dubois

► **To cite this version:**

Auriane Jones, Lionel Denis, Jérôme Fournier, Nicolas Desroy, Gwendoline Duong, et al.. Linking multiple facets of biodiversity and ecosystem functions in a coastal reef habitat. *Marine Environmental Research*, 2020, 162, pp.105092. 10.1016/j.marenvres.2020.105092 . hal-02929320

HAL Id: hal-02929320

<https://hal.science/hal-02929320v1>

Submitted on 4 Jun 2021

HAL is a multi-disciplinary open access archive for the deposit and dissemination of scientific research documents, whether they are published or not. The documents may come from teaching and research institutions in France or abroad, or from public or private research centers.

L'archive ouverte pluridisciplinaire **HAL**, est destinée au dépôt et à la diffusion de documents scientifiques de niveau recherche, publiés ou non, émanant des établissements d'enseignement et de recherche français ou étrangers, des laboratoires publics ou privés.



Distributed under a Creative Commons Attribution - NonCommercial - NoDerivatives 4.0 International License

1 **Title**

2 Linking multiple facets of biodiversity and ecosystem functions in a coastal reef habitat

3

4 **Short title**

5 Reef biogeochemical fluxes and biodiversity

6

7 **Authors**

8 Auriane G. Jones^{a,b,c}, Lionel Denis^d, Jérôme Fournier^{e,f}, Nicolas Desroy^b, Gwendoline

9 Duong^d, Stanislas F. Dubois^a

10

11 **Corresponding author**

12 Auriane G. Jones: jones.ecology@gmail.com, +33 6 22 09 42 43

13 ESE, Ecology and Ecosystems Health, Agrocampus Ouest, INRAE, 65 rue de Saint-Brieuc,

14 35042 Rennes, France

15

16 **Affiliation**

17 ^a IFREMER, Laboratoire Centre de Bretagne, DYNECO, Laboratoire d'Ecologie Benthique

18 Côtière (LEBCO), 29280 Plouzané, France

19 ^b IFREMER, Laboratoire Environnement et Ressources Bretagne nord, BP 80108, 35801

20 Dinard cedex, France

21 ^c ESE, Ecology and Ecosystem Health, AGROCAMPUS OUEST, INRA, 65 rue de Saint-

22 Brieuc, 35042 Rennes, France

23 ^d Univ. Lille, CNRS, Univ. Littoral Côte d'Opale, UMR 8187, LOG, Laboratoire

24 d'Océanologie et de Géosciences, F 62930 Wimereux, France

25 ^e CNRS, UMR 7204 CESCO, 75005 Paris, France

26 ^f MNHN, Station de Biologie Marine, BP 225, 29182 Concarneau cedex, France

27

28 **Declarations of interest: none**

29

30 **Key words**

31 Functional diversity; biogeochemical fluxes; respiration; bioturbation; community
32 composition; benthos; ecosystem engineer; *Sabellaria alveolata*; English Channel

33

34

35

36

37

38

39

40

41

42

43

44

45

46

47

48

49

50

51 1. INTRODUCTION

52 Ecosystems worldwide are experiencing increasing rates of biodiversity loss mainly caused
53 by land and sea use changes, direct resource exploitation and climate change (IPBES 2019).
54 This biodiversity crisis triggered in the 1990s a new line of work investigating the links between
55 biodiversity and ecosystem functioning and the mechanisms underpinning these relationships,
56 known today as BEF research (Hooper and Vitousek, 1997; Tilman, 1997). Focusing first on
57 terrestrial autotrophic ecosystems, many experimental studies found that an increase in plant
58 species richness led to an increase in ecosystem functions, such as primary production and
59 nutrient cycling (Cardinale et al., 2011; Hector et al., 1999; Naeem et al., 1996). Nonetheless,
60 species richness is not the unique driver of ecosystem functioning and considering the diversity
61 of functions performed by species (*i.e.* functional diversity) is also key when studying BEF
62 relationships (Hooper et al., 2005). For example, functional identity of species and functional
63 diversity among grassland species, rather than species diversity per se, together promote
64 primary production and decomposition (Mouillot et al., 2011). More generally, ecosystem
65 functioning can be promoted by a higher diversity of species and their functional traits through
66 mechanisms like resource partitioning and niche complementarity, as stated by the diversity
67 hypothesis (Tilman, 1997). Among species assemblages, dominant species and their traits can
68 also promote an ecosystem's functioning through a selection effect linked to competitive
69 differences (Cadotte, 2017), as stated by the mass ratio hypothesis (Grime, 1998).

70 In aquatic ecosystems, sediments and microorganisms are key in regulating
71 biogeochemical functions like organic matter remineralization and nutrient cycling (Jones et
72 al., 1985). Larger benthic fauna able to rework sediments (bioturbation) and/or to transfer
73 solutes (bioirrigation) also influence strongly these functions (Kristensen, 1988; Stief, 2013).
74 High densities of sediment-reworking species (*e.g.* fiddler crabs *Uca* spp. in Kristensen (2008))
75 modify the sediment resource through various biological activities like feeding, burrowing or

76 ventilation and can be considered as allogenic ecosystem engineers (Jones et al., 1994).
77 Conversely, autogenic ecosystem engineers like mangrove trees or salt marsh plants “change
78 the environment via their own physical structures”, often creating new habitats (Jones et al.,
79 1997, 1994). Many different organisms engineer marine habitats, from mollusks (*e.g.*
80 *Crassostrea virginica*) and polychaetes (*e.g. Phragmatopoma caudata*) to cnidarians (*e.g.*
81 scleractinian corals) and plants (*e.g. Zostera marina*) (Goldberg, 2013). These engineers often
82 have a positive effect on local species richness through the reduction of abiotic and biotic
83 pressures like thermal stress and predation (Romero et al., 2015; Stachowicz, 2001) and could
84 also promote, through their density, the functioning of the engineered ecosystem, a potential
85 role called the engineer effect.

86 Classically, BEF studies in aquatic ecosystems focused on soft sediments, considering
87 biogeochemical fluxes as the response variable while controlling for macrofauna species
88 richness and/or functional group richness. Such studies generally reported positive BEF
89 relationships, while stressing the role of the species’ functional identity and density (Covich et
90 al., 2004; Gamfeldt et al., 2015). In such controlled experiments, interspecific interactions like
91 resource use complementarity are limited by the manipulation of low diversity levels that
92 represent only a fraction of the local species pool (Brose and Hillebrand, 2016; Thrush and
93 Lohrer, 2012). Conversely, observational *in situ* studies can consider natural multi-trophic
94 communities along environmental gradients (Godbold and Solan, 2009) helping for example,
95 to tease apart the effects of abiotic and biotic factors on ecosystem processes (Brose and
96 Hillebrand, 2016). More generally, new hypothesis and “a more integrated empirical approach
97 to BEF research” can stem from observational studies (Thrush and Lohrer, 2012).

98 We aimed at bringing new insights on BEF relationships drawn from observations of a
99 temperate reef ecosystem built by a primary consumer, the honeycomb-worm *Sabellaria*
100 *alveolata*. Despite their ubiquity and the many ecosystem services they provide (IPBES, 2019;

101 Romero et al., 2015), bivalve and polychaete reefs are rarely investigated in the context of BEF
102 research. Studies measuring functions like respiration or calcification, mainly focus on the
103 engineer species, overlooking the role the associated organisms could have in regulating these
104 functions (Kellogg et al., 2013; Lejart et al., 2012; Newell et al., 2002; Smyth et al., 2016).
105 Natural diversity gradients often occur in ecosystems dominated by an engineer species (e.g.
106 mussels, oysters, tubicolous worms), giving us the opportunity to investigate how this particular
107 species and the associated fauna influence functions like biogeochemical fluxes (Bouma et al.,
108 2009; Jones et al., 2018; Norling and Kautsky, 2007).

109 *Sabellaria alveolata* is an intertidal ecosystem engineer distributed along the European
110 Atlantic coast from Scotland to Morocco (Muir et al., 2016). Once settled on the seabed, this
111 polychaete builds a tube using mostly bioclastic particles (Le Cam et al., 2011). When
112 environmental conditions are favorable, *S. alveolata* can form bioconstructions on rocky shores
113 or on soft sediments (Dubois et al., 2002; Gruet, 1972; Holt et al., 1998), where a diverse and
114 abundant fauna establishes (Dias and Paula, 2001; Jones et al., 2018; Porta and Nicoletti, 2009).
115 These habitats undergo natural cycles of growth (progradation) and decline (retrogradation)
116 (Curd et al. 2019) forced by abiotic factors like particle availability (Le Cam et al., 2011) and
117 hydrodynamic forces (Gruet, 1986) and by biotic factors like recruitment strength (Ayata et al.,
118 2009; Dubois et al., 2007a) and interspecific competition (Dubois et al., 2007b). These cycles
119 are mostly characterized by modifications of the reef's physical structure (Curd et al., 2019)
120 and by changes in the associated fauna in terms of richness, abundance and composition
121 (Dubois et al., 2002). Anthropogenic disturbances like trampling and coastal modifications can
122 also modify the reef's structure and the associated fauna (Desroy et al., 2011; Dubois et al.,
123 2006; Jones et al., 2018; Plicanti et al., 2016).

124 In this study, we investigated the biogeochemical functioning of a reef habitat engineered
125 by *S. alveolata* and evaluated the relative support of the engineer effect hypothesis, the diversity

126 hypothesis, and the mass-ratio hypothesis on driving key benthic processes taking place in the
127 sediments glued into bioconstructions by the tube-building activity of *S. alveolata* (*i.e.*
128 engineered sediments). First, we measured and compared the sediment-water fluxes (*i.e.*
129 oxygen, ammonium, nitrate, and nitrite) in the engineered sediments and in the surrounding soft
130 sediments. Then, using a multiple linear regression approach (model selection and effect size
131 calculation), we investigated the relative importance of the engineer itself (engineer effect
132 hypothesis) and of the macrofauna associated to the engineered sediments, in terms of
133 taxonomic or functional diversity (diversity hypothesis) and in terms of biological trait
134 dominance (mass-ratio hypothesis) on the different biogeochemical fluxes.

135

136 **2. MATERIAL AND METHODS**

137 *2.1. Study area*

138 The bay of Mont-Saint-Michel is a macrotidal bay located in the English Channel between
139 Brittany and Normandy, characterized by an intertidal zone covering over 250 km² and a mean
140 spring tide range of 14.5 m (Bonnot-Courtois et al., 2004). In its central part, the Sainte-Anne
141 reef (48°38'700N and 1°40'100W) is the largest bioconstruction in Europe, built by the
142 gregarious and tubicolous polychaete *S. alveolata* (Gruet, 1972; Holt et al., 1998). This part of
143 the bay is characterized by a high proportion of bioclastic sediments with increasing medium
144 grain size from the intertidal to the subtidal zone (Bonnot-Courtois et al., 2004). The Sainte-
145 Anne reef is located in the lower intertidal zone (between the -2 and -4 m isobaths), parallel to
146 the coastline, perpendicular to the dominant tidal currents and *ca.* 3 km from the shoreline
147 (Dubois et al., 2006; Noernberg et al., 2010). Because *S. alveolata* bioconstructions occur in
148 systems where this species finds soft sediment material to build its tube and hard substrata to
149 settle on (Curd et al. 2019), the Sainte-Anne reef is composed of a mosaic of structures built by

150 the engineer species (hereafter called engineered sediment, 32 ha in 2014, pers. obs.)
151 surrounded by soft sedimentary features (Jones et al., 2018).

152

153 2.2. *Field sampling and experimental set-up*

154 We sampled four dominant sediment typologies according to Curd et al. (2019): (1)
155 engineered sediment in prograding phase, identified by growing and expanding tubes, without
156 epibiontes (hereafter called Undisturbed Engineered Sediment or UES), (2) engineered
157 sediment in retrograding phase, identified by tubes lacking apertures, often covered by biofilm
158 and epibiontes (hereafter called Disturbed Engineered Sediment or DES), (3) soft sediment
159 composed of coarse sand (CS) with bioclastic elements and (4) soft sediment composed of fine
160 and muddy sand (MS). We sampled these four typologies 3 times over a year, according to a
161 temperature gradient: in winter (February, water temperature = 8°C), in spring (April, water
162 temperature = 12°C) and in summer (September, water temperature = 17°C). During each
163 sampling period, we randomly extracted four cores – at low tide – across a surface of *ca.* 100
164 m² of each sediment typology using either a toothed metal corer (15 cm diameter) for the
165 engineered sediment cores or 35-cm long Perspex tubes (15 cm diameter) for the soft sediment
166 cores. We immediately transferred the engineered sediment cores into 35-cm long Perspex
167 tubes (15 cm diameter), sealed all the tubes and transported them to the laboratory where we
168 placed them inside a dark refrigerated room. Prior to the coring, we collected 40 liters of
169 seawater next to the reef - during high tide - using inflatable bags to avoid bubbles that we
170 stored in a dark room at the *in situ* water temperature.

171 In the laboratory, we filled the Perspex tubes with the collected water, sealed them with
172 caps equipped with small magnetic stirrers, connected them *via* a tube to the inflatable water
173 reserve tank and incubated them respecting the *in situ* water temperature. We started the
174 incubations *ca.* 2 hours after the sampling and incubated the 16 cores sampled during each

175 campaign between 3 and 15 hours, until a loss of 30% of the initial dissolved oxygen
176 concentration measured in each core. During the incubations, we sampled 6 to 8 times both the
177 water overlying the sediment and the water from the reserve tank (control water) using a 60 ml
178 plastic syringe (see Denis et al. (2001) for further details on the incubation set up). Finally, we
179 measured the oxygen, ammonium, nitrate, and nitrite concentrations in all the water samples,
180 and we used the difference between concentration changes in the overlying water of each core
181 and control water to calculate the sediment-water fluxes.

182

183 2.3. *Flux measurements and calculations*

184 To determine oxygen concentration, we gently transferred the required volume from the 60
185 ml plastic syringe into a 10 ml glass flask using a tubing and allowing overflow from the flask
186 to avoid air bubbles. We then measured oxygen concentration using an oxygen Clark-type
187 microsensor (Revsbech, 1989) characterized by a 90 % response time of <8s, a stirring
188 sensitivity of <1.5 % and a current drift of <1 % h⁻¹ (Unisense A/S, Aarhus, Denmark, 100µm
189 tip diameter). Linear two-point calibration of each microelectrode was systematically
190 performed before and after each series of measurements. Zero oxygen current was measured in
191 the anoxic zone of an additional sediment core with muddy sediments while a 100% oxygen
192 level was calibrated using air-bubbled water. To determine the other concentrations, we filtered
193 the volume remaining in the syringe through GF/F Whatman glass fiber filters before
194 transferring them into a 20 ml polyethylene flask for ammonium analysis and a 10ml
195 polyethylene tube for nitrate and nitrite analysis. We immediately carried out the ammonium
196 analysis following the indophenol-blue method (Solórzano, 1969). We froze the remaining
197 samples and measured later on the nitrate and nitrite concentrations using a Seal autoanalyzer,
198 following the protocol of Tréguer & Le Corre (1975). We determined the fluxes by regressing
199 the change in overlying water concentration versus time and considered fluxes as null when

200 non-significant regressions (Pearson correlation, $p > 0.05$) based on changes over time were
201 less than the analytical variability. For all fluxes, we systematically applied a correction for
202 water replacement. We measured a significant oxygen consumption during all the incubations
203 ($p < 0.05$). We considered the ammonium (NH_4^+), nitrate (NO_3^-) and nitrite (NO_2^-) fluxes (from
204 the sediment to the overlying water) from the following cores as null; two spring CS cores for
205 the NH_4^+ fluxes, all the summer MS cores for the NO_3^- fluxes and two spring MS cores, one
206 summer MS core and one summer CS core for the NO_2^- fluxes. Finally, we expressed the nitrate
207 and nitrite fluxes of each core as a sum we called nitrate + nitrite flux (NO_{2+3}) and considered
208 the oxygen flux as going from the overlying water to the sediment, hereafter called the sediment
209 oxygen demand (SOD).

210

211 2.4. *Macrofauna taxonomic and functional diversity*

212 At the end of each incubation, we fixed the sediment cores using a 5 % formaldehyde
213 solution, before sieving them through a 1-mm square mesh. We sorted the macrofauna (>1 mm)
214 and identified it to the lowest taxonomic level, often species level (except for Nemertean,
215 Nematodes and Tubificoides, see Table S1). For each core, we measured the abundance and the
216 ash-free dry weight (AFDW – 4 hours at 550°C) of each taxonomic group including the
217 engineer species *S. alveolata* and then standardized the different measurements taken for each
218 core (fluxes, macrofauna abundance and biomass) to unit surface. First, we characterized the
219 macrofauna according to each species taxonomic identity, before calculating Hill's indices (*i.e.*
220 the number equivalents of three diversity indices), always including *S. alveolata* (Hill, 1973):
221 the species richness (SR), the exponential of Shannon-Wiener (\log_e) calculated using either the
222 abundance ($N1_{ab}$) or the biomass ($N1_{biom}$) and the inverse of Simpson's dominance calculated
223 using either the abundance ($N2_{ab}$) or the biomass ($N2_{biom}$). Hill's indices are recommended for

224 the study of benthic communities (Gray, 2000) and have the “doubling” property, making their
 225 interpretation more straightforward than the raw Shannon-Wiener and Simpson dominance
 226

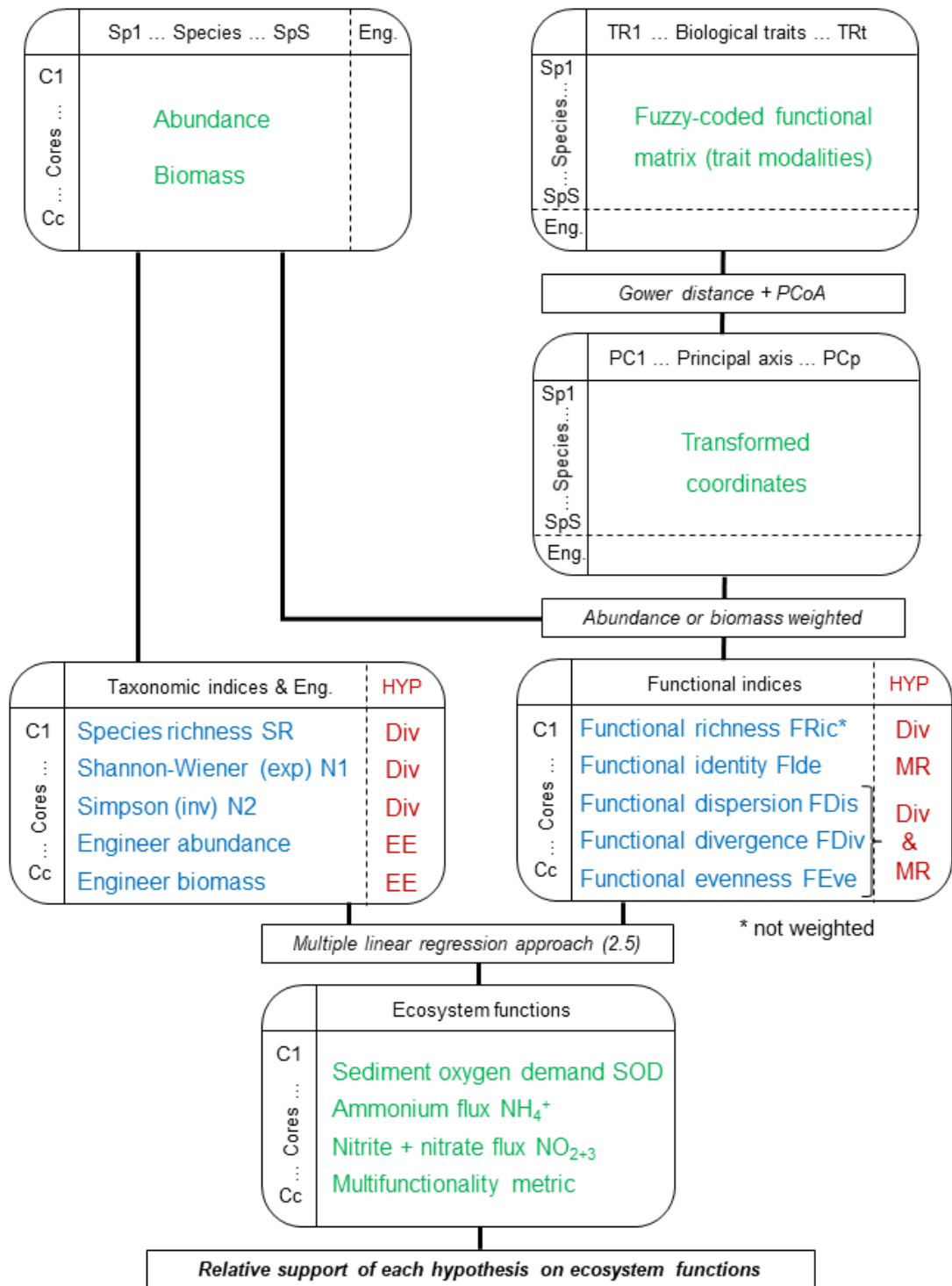
227 **Table 1.** Macrofauna biological traits and associated modalities used to calculate the functional
 228 diversity indices. For each trait, we indicated the macrofauna processes linked to organic matter
 229 remineralization and nutrient cycling, along with the macrofauna processes linked to the
 230 ecosystem functions via microorganism processes.

Trait and associated modalities	Direct macrofauna processes	Via microorganism processes	References
Maximum size (literature, mm): <10 [10-50[[50-100[[100-200[>200	respiration, excretion of DIN	egestion of POM via remineralization, transport of solutes and O ₂ via nitrification, denitrification	Hildrew et al. (2007); Kristensen (1988); Shumway (1979); Vanni (2002)
Daily movement capacity: No movement Low (<1 m) Medium (1-10 m) High (>10 m)	respiration, excretion of DIN	transport of solutes and O ₂ via nitrification, denitrification, remineralization	Kristensen (1988); Queirós et al. (2013); Shumway (1979)
Sediment reworking: Epifauna Surficial modifiers Upward and downward conveyors Biodiffusors Regenerators		transport of solutes and O ₂ via nitrification, denitrification, remineralization	Janson et al. (2012); Queirós et al. (2013); Solan et al. (2004); Thrush et al. (2006)
Feeding mode: Suspension feeder Surface deposit feeder Sub-surface deposit feeder Predator-scavenger Grazer	respiration, excretion of DIN, ingestion of POM	egestion of POM via remineralization	Janson et al. (2012); Kristensen (1988); Thrush et al. (2006)
Bathymetric preference: Intertidal Subtidal		informs indirectly on the engineered sediment’s thermal properties which can mediate microorganism processes	Gutiérrez and Jones (2006)

231 DIN: dissolved inorganic nitrogen, POM: particulate organic matter

232 indices (Hill, 1973). The indices N1 and N2 both increase when the sample diversity increases
233 but N1 is sensitive to the abundance or biomass variations of rare or uncommon species while
234 N2 is sensitive to the variations of the most common species. Then, we characterized the
235 macrofauna according to a set of biological traits (five categorical traits each divided into
236 modalities) known to directly or indirectly affect individual processes (“effect traits” *sensus*
237 Lavorel & Garnier (2002)), such as aerobic respiration, which themselves affect benthic
238 ecosystem functions such as nitrogen cycling and organic matter remineralization (Table 1).
239 These ecosystem functions are estimated by measuring oxygen and solute fluxes (*i.e.* NH_4^+ ,
240 NO_3^- , NO_2^-) between the sediment and the overlying water. We used the two main components
241 of the bioturbation potential (Queirós et al., 2013), mobility and sediment reworking, rather
242 than the bioturbation potential per se because both components are influenced by habitat
243 structure (Godbold et al., 2011), a characteristic differing between UES and DES zones of the
244 reef (Curd et al., 2019; Jones et al., 2018). Furthermore, transferring bioturbation potential
245 across space and time is only possible if the species body size is constant (Queirós et al., 2013),
246 which was not the case since we sampled across three different periods.

247 Some species present different modalities for certain traits like *Carcinus maenas*, which can
248 behave as a grazer and as a predator-scavenger (2 modalities in the feeding mode trait). To take
249 into account this intraspecific variability, we fuzzy coded the categorical traits by assigning a
250 value between 0 (no affinity) and 3 (strict affinity) to each modality of a given trait depending
251 on the species affinity for the modality, with 1 and 2 indicating intermediate affinities (Chevenet
252 et al., 1994). The sum of the values attributed to all the modalities of a given trait was always
253 equal to three except for the tidal position, which could be equal to four if the species had an
254 equal affinity for the intertidal and subtidal modalities. We recovered most of the information
255 on polychaete feeding mode and daily movement capacity from Fauchald & Jumars (1979) and
256 Jumars et al. (2015). The rest was recovered from peer-reviewed journals



257

258 **Figure 1.** Framework used to study the relative support of the diversity hypothesis (Div), the
 259 mass ratio hypothesis (MR) and the engineer effect hypothesis (EE) on ecosystem functions
 260 (here biogeochemical fluxes) in the context of a community structured by an ecosystem
 261 engineer (Eng.). Each index in blue is used to test a specific hypothesis (HYP) in red and all
 262 the indices along with the water temperature, were first considered as explanatory variables in
 263 the multiple linear regression approach detailed in part 2.5. Adapted from Villéger et al. (2008).

264 (Guerra-García et al., 2014; Navarro-Barranco et al., 2013) and biological trait databases
265 (Marine species identification portal, BIOTIC).

266 Using the biological traits matrix defined for the 43 species identified in the UES and DES
267 cores (n = 24), we calculated several functional indices following the framework detailed in
268 Figure 1 and using the R packages presented in Table 2. We used the Gower distance to
269 calculate the functional distance between each pair of species and then performed a principal
270 coordinate analysis (PCoA) on the distance matrix (Laliberté and Legendre, 2010; Villéger et
271 al., 2008) to represent each species in a multidimensional functional space, each dimension
272 (PCoA axis, 42 axes in total) being a combination of traits. Finally, we calculated for each core,
273 several functional diversity and identity indices using different data types (Table 2) and
274 weighted each index (except functional richness) by species relative abundance (ab in subscript)
275 or relative biomass (biom in subscript) (Fig. 1). *Sabellaria alveolata* was always included in
276 the data sets used to calculate the indices. Functional richness was standardized by the 'global'
277 functional richness (including all species recorded in the UES and DES cores) to constrain it
278 between 0 and 1 (Laliberté and Legendre, 2010).

279

280 2.5. *Statistical analyses*

281 First, we tested the effect of sediment typology (four levels: CS, MS, UES and DES),
282 sampling period (three levels: spring, summer and winter) and their interaction on the different
283 fluxes (SOD, NH_4^+ and NO_{2+3}) using an analysis of variance (ANOVA) with a two-way crossed
284 balanced design. If the interaction term was significant for a flux, we performed Tukey HSD
285 post-hoc tests to disentangle which sediment typology x sampling period cores presented
286 significantly higher or lower fluxes than others. After running the ANOVAs, we checked each
287 model's residuals for normality using a histogram and for homoscedasticity by plotting them
288 against the predicted values (Zuur et al., 2010).

289 **Table 2.** Definition and associated information (data type, key references, R functions and weighting procedure) on the five functional indices
 290 (diversity and identity). The first four PCoA axes represent 60% of the total inertia. See Figure 4 for a graphical illustration of each index.

Functional indices	Name	Definition	Data type	Unweighted or weighted	Key references	R function
Functional identity	FIde	Weighted average position on the selected functional space axis (PCoA axis)	PCoA axis 1, 2 or 3	Weighted by abundance or biomass	Mouillot et al. (2013)	multidimFD
Functional richness	FRic	Multidimensional functional space filled by all species in a community	PCoA axes 1 to 4	Unweighted	Villéger et al. (2008); Laliberté and Legendre (2010)	dbFD
Functional dispersion	FDis	Weighted average distance to the weighted average mean trait values of the community	Uncorrected functional distance matrix	Weighted by abundance or biomass	Laliberté and Legendre (2010)	dbFD
Functional divergence	FDiv	Weighted average deviation of the Euclidian distance between the position of all the species in the functional space and the unweighted center of gravity of the vertices of the convex hull	PCoA axes 1 to 4	Weighted by abundance or biomass	Villéger et al. (2008)	dbFD
Functional evenness	FEve	Regularity of abundance or biomass distributions in the functional space along the shortest minimum spanning tree linking all the species	PCoA axes 1 to 42	Weighted by abundance or biomass	Villéger et al. (2008); Laliberté and Legendre (2010)	dbFD

291 sediment core a multifunctionality metric using the mean of the four standardized fluxes (mean
292 = 0 and SD = 1), to give them the same weight (Mouillot et al., 2011).

293 Then, to estimate the importance of macrofauna vs meiofauna + microorganisms in organic
294 matter processing, we calculated the macrofauna-normalized SOD ($\text{mmol O}_2 \cdot \text{day}^{-1} \cdot \text{g AFDW}^{-1}$)
295 1) for each core by dividing the daily oxygen consumption ($\text{mmol O}_2 \cdot \text{day}^{-1}$) by the total
296 macrofauna biomass (g AFDW). Values inferior to 1 indicate processes are predominantly
297 driven by macrofauna whereas values superior to 1 indicate processes are predominantly driven
298 by meiofauna and microorganisms (Stenton-Dozey et al., 2001 in Clough et al., 2005). A
299 multifunctionality metric was also calculated for each engineered sediment core as the mean of
300 the four fluxes after standardizing each of them (mean of 0 and standard deviation of 1) to give
301 them the same weight (Mouillot et al., 2011).

302 Finally, we implemented a multiple linear regression approach (ordinary least-square
303 regressions) to determine the relative importance of (1) water temperature, (2) the engineer *S.*
304 *alveolata* (engineer effect hypothesis), (3) macrofauna diversity in terms of species or
305 biological traits (diversity hypothesis) and (4) the functional traits of the dominant species
306 (mass-ratio hypothesis) on the four ecosystem functions measured in the engineered sediments.
307 Each index presented in Figure 1 is used to test one hypothesis, except FDis, FDiv and FEve,
308 which are used to test the diversity and mass-ratio hypotheses (Mokany et al., 2008), as their
309 values are driven by macrofauna traits and macrofauna abundance or biomass. We considered
310 the 24 incubated engineered sediment cores as statistically independent replicates because the
311 cores were physically isolated from each other during the flux measurements (independent
312 incubations) and the processes we measured take place at spatial scales inferior to the *in situ*
313 distance separating two cores (Hewitt et al., 2005). Indeed, the cores sampled in the UES and
314 DES sediment typologies were extracted from different engineered sediment patches across a
315 surface of *ca.* 100 m² and most of the engineered sediment benthic macrofauna being sessile or

316 presenting a low mobility, their movements are constrained to a given engineered sediment
317 patch (Table 1, Fig. 4 and 5).

318 First, we reduced the number of explanatory variables, previously standardized (Schielzeth,
319 2010), to consider in the multiple linear regressions by removing variables that were highly
320 correlated ($|r| > 0.8$, Spearman correlations) (Godbold and Solan, 2009). We removed $N2_{ab}$ and
321 $N2_{biom}$ as they were highly correlated with $N1_{ab}$ ($r = 0.98$) and $N1_{biom}$ ($r = 0.98$), respectively,
322 $FIde2_{ab}$ and $FIde2_{biom}$ as they were highly correlated with $FIde1_{ab}$ ($r = -0.97$) and $FIde1_{biom}$ ($r =$
323 -0.87), respectively and $FDiv_{ab}$ and $FDiv_{biom}$ as they were highly correlated with $FDis_{ab}$ ($r = -$
324 0.85) and $FDis_{biom}$ ($r = -0.90$), respectively. After this step, we had one environmental variable
325 (temperature), two variables associated to the engineer effect hypothesis (*S. alveolata*
326 abundance and biomass), four variables associated to the diversity hypothesis (SR, $N1_{ab}$, $N1_{biom}$
327 and FRic), four variables associated to the mass-ratio hypothesis ($FIde1_{ab}$, $FIde1_{biom}$, $FIde3_{ab}$
328 and $FIde3_{biom}$) and four variables associated to the diversity and mass ratio hypotheses ($FDis_{ab}$,
329 $FDis_{biom}$, $FEve_{ab}$ and $FEve_{biom}$).

330 Secondly, we built first and second-degree polynomial regressions between each
331 explanatory variable and each ecosystem function, as preliminary inspections of the biplots
332 indicated the presence of quadratic relations (Thrush et al., 2017). Prior to this second step, we
333 squared the 15 remaining explanatory variables to build raw second-degree polynomial
334 regressions and the second-degree terms were standardized to improve the interpretability of
335 the multiple linear regression coefficients (Schielzeth, 2010). Regarding temperature, we only
336 considered first-degree linear regressions, as water temperature inside small ranges (here 9°C)
337 will have positive effects on biogeochemical fluxes such as SOD, according to the Q10 of 2
338 general relation (Herbert, 1999; Hildrew et al., 2007; Thamdrup et al., 1998).

339 Thirdly, the variable associated to each hypothesis that had a significant effect on a given
340 ecosystem function ($p < 0.05$) and explained the highest amount of ecosystem function

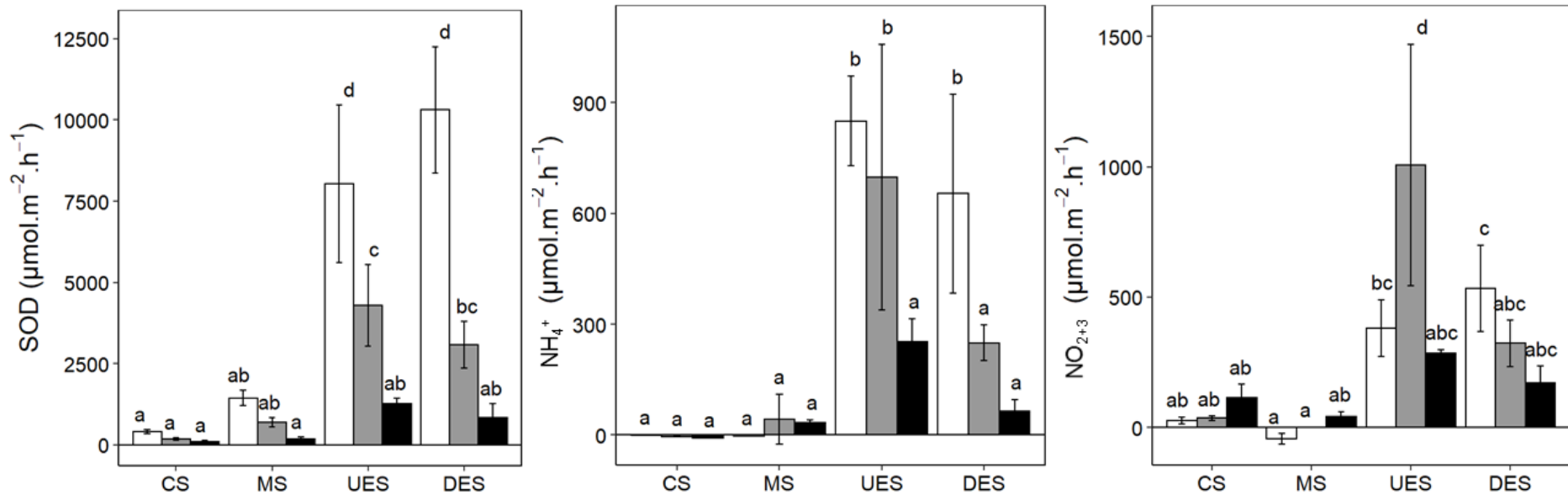
341 variability (adjusted R^2) was included in the four initial multiple linear models. The following
342 explanatory variables were considered in each initial multiple linear model: for SOD,
343 temperature, *S. alveolata* biomass (first-degree), FId_{1ab} (second-degree) and $FDis_{ab}$ (second-
344 degree); for NH_4^+ , temperature, *S. alveolata* biomass (first-degree), SR (first-degree), FId_{1ab}
345 (first-degree) and $FDis_{ab}$ (second-degree); for NO_{2+3} , temperature, *S. alveolata* abundance
346 (first-degree), NI_{ab} (first-degree) and $FEve_{ab}$ (second-degree); for the multifunctionality metric,
347 temperature, *S. alveolata* biomass (first-degree), SR (first-degree), FId_{1biom} (first-degree) and
348 $FDis_{ab}$ (second-degree).

349 Finally, to determine the minimal adequate models (final multiple linear models), we
350 selected the subset of predictors that minimized the Akaike information criterion (AIC) using
351 the 'ols_step_best_subset' function from the 'olsrr' package. If two models had AIC differences
352 of less than 2, we chose the one with the lowest Mallows' C_p to select the most parsimonious
353 model (Godbold and Solan, 2009). Before running the model selection procedure, we removed
354 the explanatory variables that presented high levels of collinearity based on a threshold of the
355 variance inflation factor of 10. For SOD and NH_4^+ , we removed FId_{1ab} , which was highly
356 correlated with $FDis_{ab}$ ($r = 0.99$) and defined reduced multiple linear models. After running each
357 model (initial, reduced, and final multiple linear regressions), we checked the residuals for
358 normality using a histogram and for homoscedasticity by plotting them against the predicted
359 values (Zuur et al., 2010). To estimate the independent effect of each selected predictor on a
360 given ecosystem function, we calculated the standardized partial regression coefficients and
361 represented this independent effect using partial linear regression plots (Schielzeth, 2010). We
362 considered a significance level of 0.05 for all the tests.

363

364 3. RESULTS

365 3.1. *Effect of sediment typology and sampling period on the different fluxes*



366

367 **Figure 2.** Sediment oxygen demand (SOD), ammonium flux (NH_4^+) and the sum of nitrate and nitrite fluxes (NO_{2+3}) measured for the four sediment
 368 typologies (mean \pm SD, n = 4), coarse sand (CS), muddy sand (MS), undisturbed engineered sediments (UES) and disturbed engineered sediments
 369 (DES) in spring (white), summer (grey) and winter (black). The results of the post-hoc tests performed after the two-way crossed ANOVA
 370 (sediment typology x sampling period) are presented as letters above each barplot, considering a p-value of 0.05.

371 Visually, the SOD, NH_4^+ and NO_{2+3} fluxes appeared higher in the undisturbed (UES) and
372 disturbed (DES) engineered sediments compared to the coarse (CS) and muddy (MS) sediments
373 across the three sampling periods. The engineered sediment fluxes appeared maximal in spring
374 (Fig. 2 and Table S2). The mean SOD ranged from a minimum of $105 \mu\text{mol}\cdot\text{m}^{-2}\cdot\text{h}^{-1}$ in winter
375 for the CS cores to a maximum of $10\,309 \mu\text{mol}\cdot\text{m}^{-2}\cdot\text{h}^{-1}$ in spring for the DES cores. Sediment
376 typology ($F(3,36) = 68.83, p < 0.001$), sampling period ($F(2,36) = 81.95, p < 0.001$) and their
377 interaction ($F(6,36) = 20.96, p < 0.001$) had statistically significant effects on the SOD. The CS
378 cores and the winter MS cores had the lowest SOD while the spring UES and DES cores and
379 the summer UES cores had, respectively the first and second highest SOD. The spring and
380 summer MS cores, the winter UES and DES cores and the summer DES cores had intermediate
381 SOD (spring and summer MS and winter UES and DES \leq summer DES \leq summer UES, Fig.
382 2).

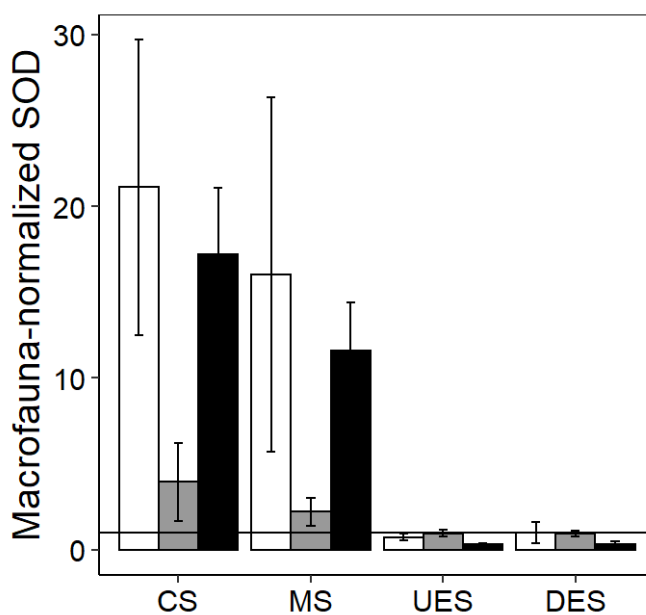
383 The mean NH_4^+ fluxes ranged from slightly negative (between -7.9 and $-0.8 \mu\text{mol}\cdot\text{m}^{-2}\cdot\text{h}^{-1}$)
384 for all the CS cores and for the MS cores in spring to above $200 \mu\text{mol}\cdot\text{m}^{-2}\cdot\text{h}^{-1}$ for all the UES
385 cores and for the spring and summer DES cores with the maximum values measured in the
386 spring UES cores ($850.40 \pm 121.79 \mu\text{mol}\cdot\text{m}^{-2}\cdot\text{h}^{-1}$). Sediment typology ($F(3,36) = 51.14, p <$
387 0.001), sampling period ($F(2,36) = 17.72, p < 0.001$) and their interaction ($F(6,36) = 7.26, p <$
388 0.001) had statistically significant effects on the NH_4^+ fluxes. All the CS, MS, the winter UES
389 and the spring and winter DES cores had significantly lower NH_4^+ fluxes than the spring and
390 summer UES cores and the spring DES cores (Fig. 2).

391 All the NO_{2+3} fluxes were on average positive except in the spring MS cores ($-43.7 \mu\text{mol}\cdot\text{m}^{-2}\cdot\text{h}^{-1}$)
392 $^2\cdot\text{h}^{-1}$). The summer MS cores had mean NO_{2+3} fluxes near zero ($0.2 \mu\text{mol}\cdot\text{m}^{-2}\cdot\text{h}^{-1}$) while the rest
393 of the soft sediment cores had mean fluxes between 26.0 and $114.2 \mu\text{mol}\cdot\text{m}^{-2}\cdot\text{h}^{-1}$. All the
394 engineered sediment cores had mean fluxes above $170.6 \mu\text{mol}\cdot\text{m}^{-2}\cdot\text{h}^{-1}$ with the maximum values
395 measured in the summer UES cores ($1\,006.9 \pm 463.8 \mu\text{mol}\cdot\text{m}^{-2}\cdot\text{h}^{-1}$). Sediment typology ($F(3,36)$

396 = 35.89, $p < 0.001$), sampling period ($F(2,36) = 6.41$, $p = 0.004$) and their interaction ($F(6,36)$
 397 = 9.17, $p < 0.001$) had statistically significant effects on the NO_{2+3} fluxes. The spring and
 398 summer MS cores presented the lowest NO_{2+3} fluxes while the summer UES and the spring
 399 DES cores presented, respectively the first and second highest NO_{2+3} fluxes. The rest of the
 400 cores presented intermediate NO_{2+3} fluxes (winter CS and MS \leq winter UES and DES and
 401 spring DES \leq spring UES, Fig. 2).

402 Calculation of the macrofauna-normalized SOD for each core indicated that meiofauna and
 403 microorganisms predominantly drove organic matter processing in the CS and MS
 404 (macrofauna-normalized SOD $\gg 1$). Differently, macrofauna was the principal driver of
 405 organic matter processing in the UES and DES (Fig. 3).

406



407

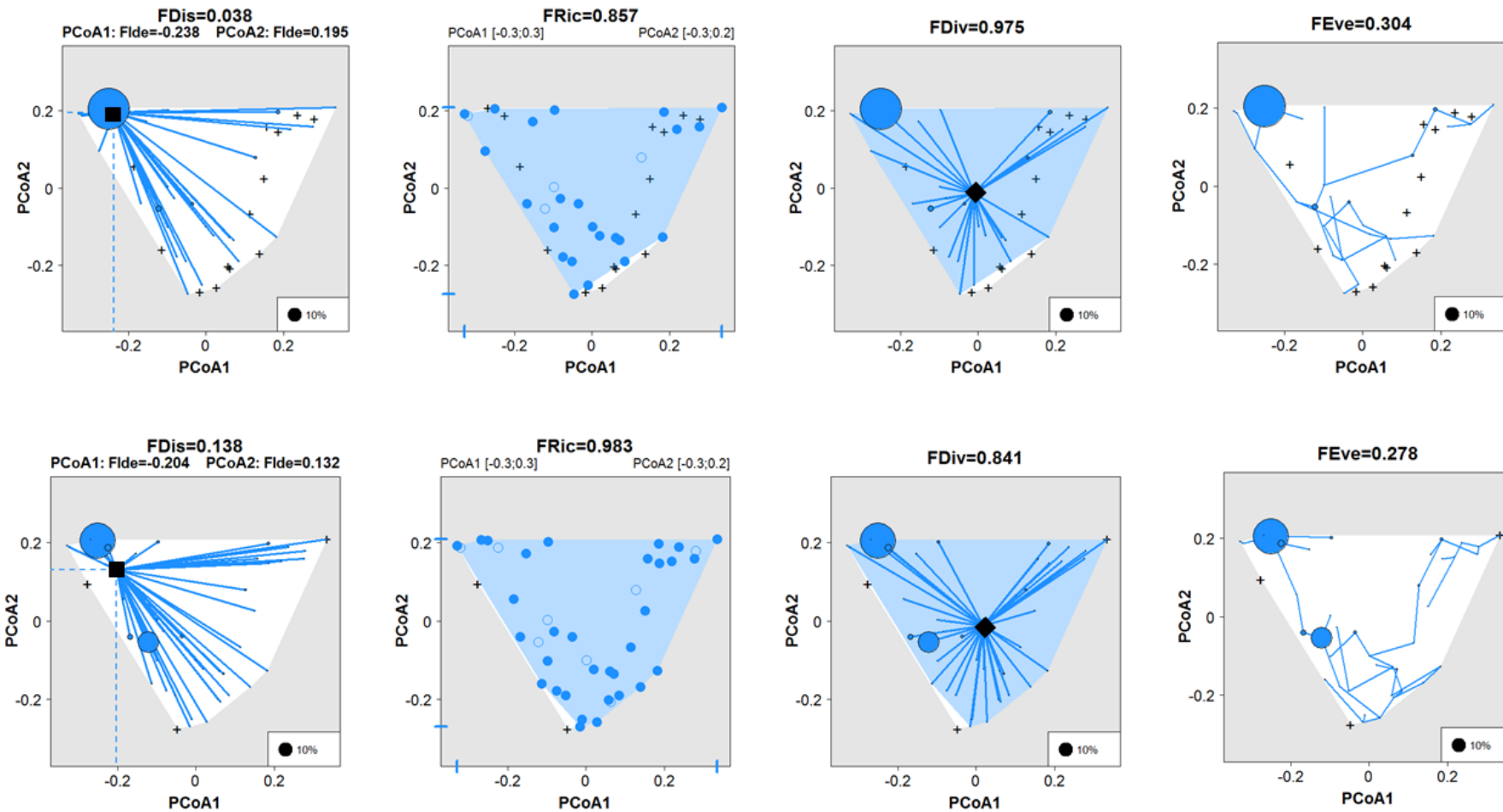
408 **Figure 3.** Macrofauna-normalized sediment oxygen demand (SOD) in $\text{mmol O}_2 \cdot \text{day}^{-1} \cdot \text{g}$
 409 AFDW^{-1} (mean \pm SD, $n = 4$) calculated for the four sediment typologies, coarse sand (CS),
 410 muddy sand (MS), undisturbed engineered sediments (UES) and disturbed engineered
 411 sediments (DES) in spring (white), summer (grey) and winter (black). The horizontal line
 412 represents a macrofauna-normalized SOD value of one. To improve readability, we removed
 413 one winter CS core with a macrofauna-normalized SOD above 30 ($140.5 \text{ mmol O}_2 \cdot \text{day}^{-1} \cdot \text{g}$
 414 AFDW^{-1}).

415 3.2. *Functional diversity and identity indices*

416 Each functional index weighted by biomass was significantly and positively correlated with
417 its abundance-weighted version, except FEve. Functional richness, FDis, FDiv, FIde1 and
418 FIde2 weighted by biomass and abundance presented values intricately linked to the engineered
419 sediment types (UES vs DES). The other functional indices appeared to be completely
420 independent from the engineered sediment type (FEve) or weakly linked to it (FIde3).

421 As an illustration (Fig. 4), we calculated the different functional indices using the mean
422 macrofauna biomass across all the DES (n = 12) and all the UES cores (n = 12). The mean DES
423 core had a higher FRic (0.98) than the mean UES core (0.86) indicating there were more
424 functionally dissimilar species in DES than in UES. Functional dispersion followed the same
425 pattern with a higher value in the mean DES core (0.14) than in the mean UES core (0.04). If a
426 species dominates an assemblage (e.g. *S. alveolata* in UES, Table S1), it will attract the
427 weighted-mean position of the assemblage and the FDis will be small. Differently, if two
428 species have high abundances or biomasses and are distant in the functional space (i.e.
429 functionally dissimilar), like *S. alveolata* and the crustacean *Porcellana platycheles* in the DES
430 cores (Fig. 5 and Table S1), both will attract the weighted-mean position of the assemblage and
431 the FDis will be higher. Functional divergence was higher in the mean UES (0.98) than in the
432 mean DES core (0.84) because *S. alveolata*, which presents trait modalities very different from
433 the “average species” represented by the unweighted center of gravity of the convex hull
434 vertices (Fig. 5), dominates the UES cores while it dominates less the DES cores (Table S1).

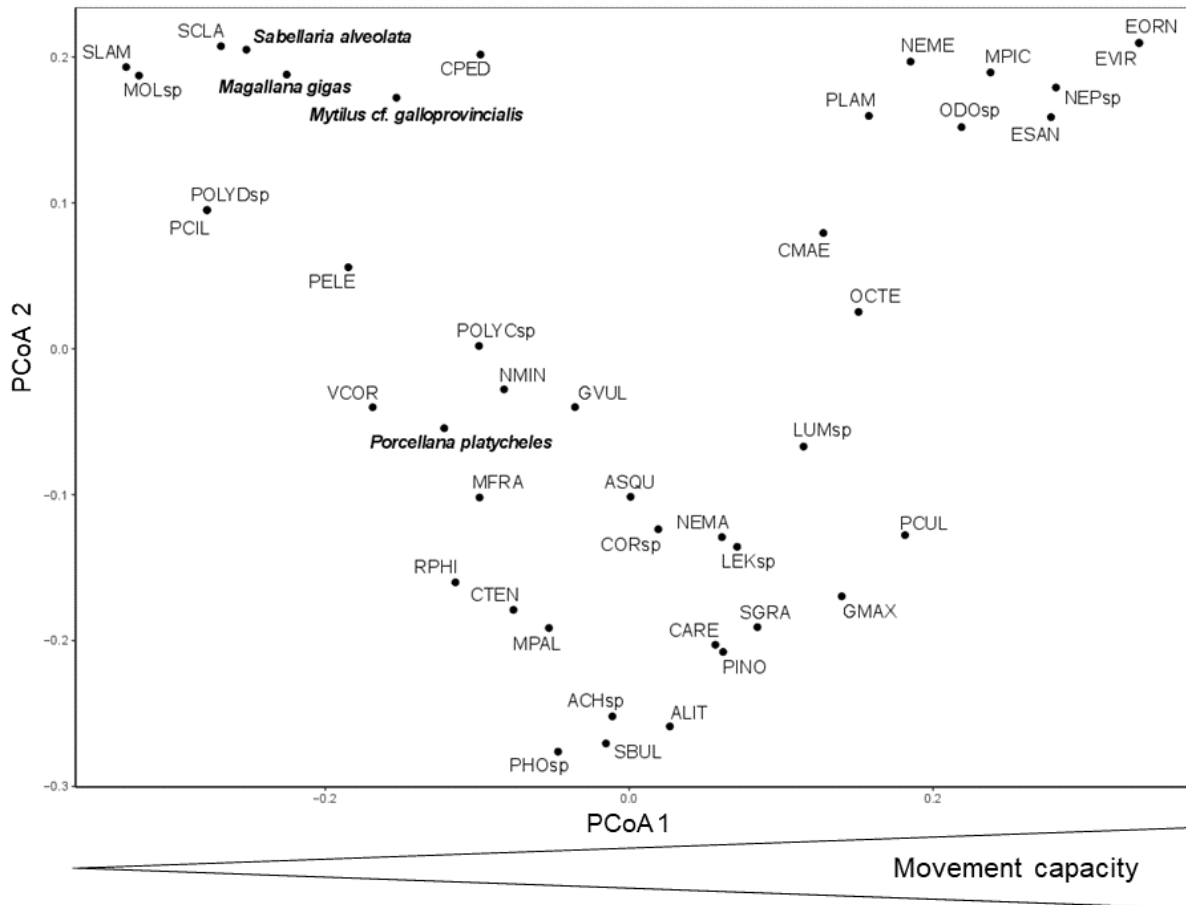
435 The mean UES core was characterized by negative FIde1 (-0.24) and positive FIde2 (0.19)
436 while the mean DES core was characterized by higher and negative FIde1 (-0.20) and by lower
437 and positive FIde2 (0.13). The first PCoA axis is mainly associated to a daily movement
438 capacity gradient with negative values corresponding to species presenting none to low
439 movement capacities (e.g. *Sabellaria alveolata*) and higher values corresponding to



440

441 **Figure 4.** Two-dimensional illustration of the five functional indices (functional dispersion = FDis, functional identity = FIdes, functional richness = FRic, functional divergence = FDiv, functional evenness = FEve) based on the species identified in the 12 undisturbed (top line) and 12 disturbed
 442 = FRic, functional divergence = FDiv, functional evenness = FEve) based on the species identified in the 12 undisturbed (top line) and 12 disturbed
 443 (bottom line) engineered sediment cores. The black crosses indicate species absent from an engineered sediment type but present in the global pool
 444 of species. Except for FRic, the dots are proportional to each species' mean biomass. In the FDis panels, the black squares and dashed lines represent

445 the weighted-mean position of the species in the multidimensional space and the weighted-mean positions of the species on the first and second
446 axis (FIde1 and FIde2), respectively. In the FRic panels, the colored convex polygons represent the projection of the multidimensional convex hull
447 in 2D, the filled symbols represent the species used as vertices in the multidimensional space and the bold bars on the axes represent the minimum
448 and maximum values on each axis. In the FDiv panels, the black diamonds represent the center of gravity of the vertices. In the FEve panels, the
449 blue lines represent the minimum spanning tree linking all species in the multidimensional space.



450
 451 **Figure 5.** Position, on the first two axes of the functional space, of all the species present at the
 452 global engineered sediment level and identified by their full or abbreviated names (see Table
 453 S1). *Sabellaria alveolata* is the engineer species while *Porcellana platycheles* is the second
 454 dominant species in the disturbed engineered sediment cores. *Magallana gigas* and *Mytilus cf.*
 455 *galloprovincialis* are two other engineer species present as epibionts on the engineered
 456 sediments.

457
 458 increasingly mobile species (e.g. errant polychaetes such as *Eulalia viridis*, EVIR) (Fig. 5). The
 459 second PCoA axis is mainly associated to the sediment reworking trait with positive values
 460 generally corresponding to epifauna (e.g. *Magallana gigas*) and biodiffusors (e.g. Nemerteans,
 461 NEME), values close to 0 corresponding to upward and downward conveyors (e.g.
 462 *Mediomastus fragilis*, MFRA and *Pygospio elegans*, PELE) and negative values corresponding
 463 to surficial modifiers (e.g. *Lekanesphaera* sp., LEKsp) (Fig. 5). Consequently, functional
 464 identity values on the first two PCoA axes can bring direct indications on which modalities are

465 key in driving the different ecosystem functions. The other biological traits (size, feeding mode
466 and bathymetric preference) were not associated with a specific PCoA axis.

467

468 3.3. *Relative importance of macrofauna and temperature on the engineered sediment* 469 *biogeochemical functioning*

470 The minimal adequate models contained three or four predictors and explained *ca.* 70% of
471 the ecosystem function variability (Table 3). All the models contained water temperature, a
472 predictor associated to the engineer effect hypothesis (*S. alveolata* biomass or abundance) and
473 a predictor associated to both the diversity and mass-ratio hypotheses (FDis_{ab} or FEve_{ab}).
474 Furthermore, FDis_{ab} and FIdel_{ab} appeared correlated at 0.99 (Spearman correlation) indicating
475 that when FDis_{ab} increases, the abundance of species with medium to high movement capacities
476 also increases (Figure S3). One UES core sampled in summer was closer to the summer DES
477 cores than to the other summer UES cores because of a higher FDis_{ab} and a lower engineer
478 abundance. Nonetheless, the fluxes of this unexpectedly different core in terms of macrofauna
479 characteristics were in line with the partial linear regressions (Fig. 6), which seems to indicate
480 our minimal adequate models are not the result of an UES/DES dichotomy.

481 a. Engineer effect hypothesis

482 Based on the standardized slopes also called standardized partial regression coefficients or
483 effect sizes (β), the engineer had a positive effect on the four functions (Fig. 6). Engineer
484 biomass (mean = 125, SD = 94) was the predictor with the strongest effect on the SOD (mean
485 = 4640, SD = 3750) and NH₄⁺ (mean = 462, SD = 330) fluxes, holding all the other predictors
486 of each model statistically constant. An increase by one population SD of *S. alveolata* biomass
487 increases the SOD and NH₄⁺ fluxes by 0.63 and 0.59 population SD, respectively (Table 3).
488 Considering the multifunctionality metric model, engineer biomass had an effect of comparable
489 magnitude to FDis_{ab} (Table 3). Finally, engineer abundance (mean = 4765, SD = 13 936) was

490 **Table 3.** Minimal adequate models (ordinary least-square regressions) explaining the
 491 standardized ecosystem functions (sediment oxygen demand (SOD), ammonium flux (NH₄⁺),
 492 sum of nitrate and nitrite fluxes (NO₂₊₃) and the multifunctionality metric). We expressed the
 493 slope estimates as effect sizes (β) to compare their relative effects on each function.

	df	RSE	F statistic	β	P
SOD adjusted R² = 0.73					
Model	3		21.3		< 0.001
Error	20	0.52			
Biomass				0.63	< 0.001
FDis _{ab} ²				-0.31	0.025
Temperature				0.23	0.048
NH₄⁺ adjusted R² = 0.69					
Model	3		18.4		< 0.001
Error	20	0.55			
Biomass				0.59	< 0.001
Temperature				0.45	0.001
FDis _{ab}				-0.35	0.011
NO₂₊₃ adjusted R² = 0.70					
Model	3		19.0		< 0.001
Error	20	0.55			
Abundance				0.62	< 0.001
Temperature				0.30	0.031
FEve _{ab}				-0.25	0.076
Multifunctionality metric adjusted R² = 0.73					
Model	4		17.0		< 0.001
Error	19	0.51			
Temperature				0.52	< 0.001
Biomass				0.37	0.021
FDis _{ab}				-0.38	0.008
FDis _{ab} ²				-0.32	0.035

494 df: degree of freedom, RSE: Residual standard error, Abundance: *S. alveolata* abundance,
 495 Biomass: *S. alveolata* biomass, FEve: functional evenness, FDis: functional dispersion. The
 496 subscripts ab indicates that the index was weighted using species abundance.

497

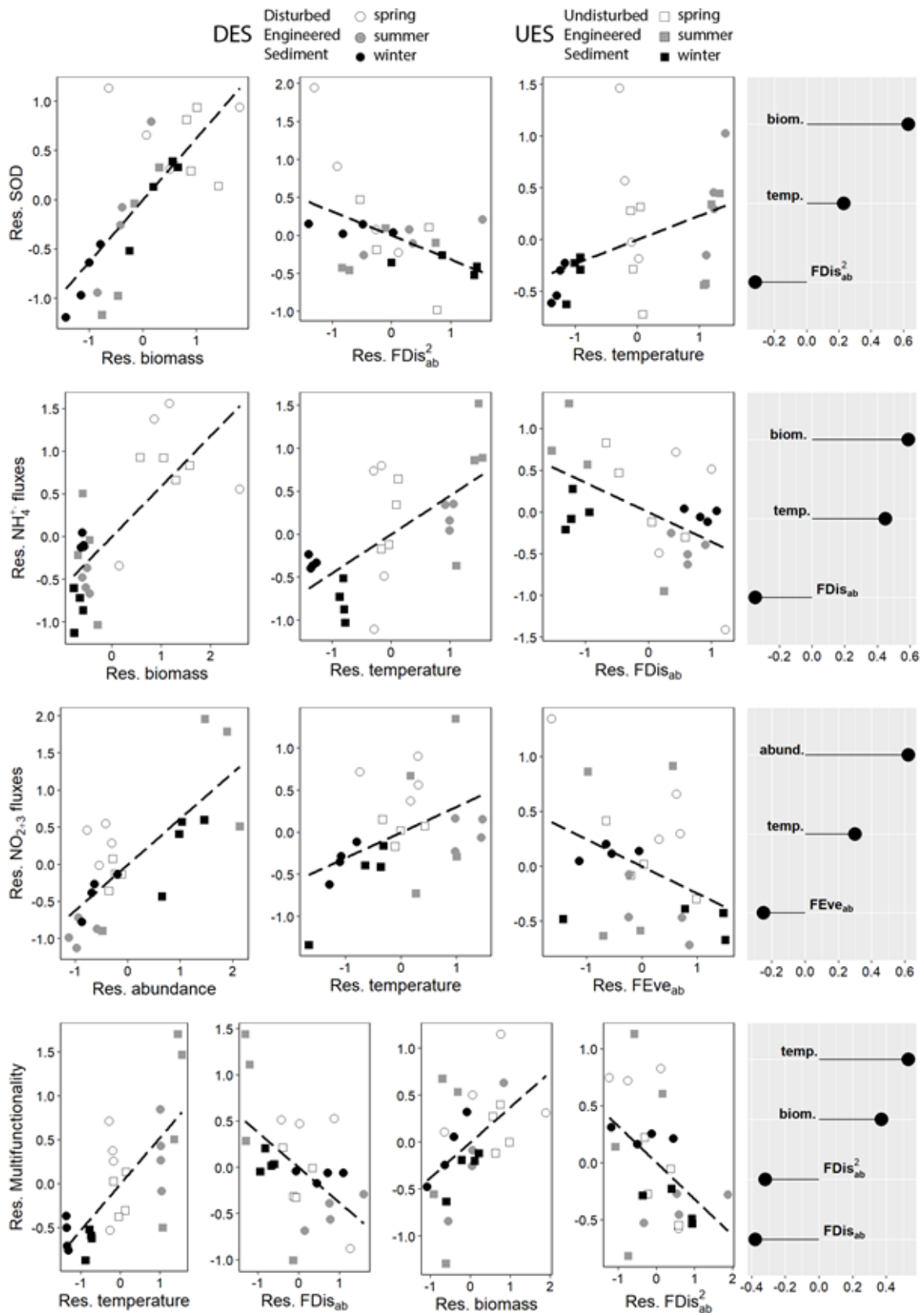
498 the predictor with the strongest effect on the NO₂₊₃ fluxes (mean = 450, SD = 334), holding all
 499 the other predictors of the model statistically constant (Table 3).

500 b. Diversity and mass-ratio hypotheses

501 Two functional indices weighted by abundance were retained in the minimal adequate
502 models, FDis (mean = 0.18, SD = 0.11) and FEve (mean = 0.61, SD = 0.11), and both predictors
503 always presented negative standardized slopes (Fig. 6). The functional dispersion displayed a
504 simple linear effect on the NH_4^+ fluxes, a simple quadratic effect (concave form) on the SOD
505 and a more complex quadratic effect on the multifunctionality metric (*i.e.* concave form with
506 low values of FDis_{ab} eliciting higher values of the multifunctionality metric than high values of
507 FDis_{ab}). It was the predictor with the weakest effect on the NH_4^+ fluxes and with the second
508 strongest effect on the SOD. The functional evenness displayed a simple linear effect on the
509 NO_{2+3} fluxes and was the predictor with the weakest effect, holding all the other predictors of
510 the model statistically constant (Table 3).

511 c. Water temperature

512 Based on the standardized partial regression coefficients, the water temperature (mean =
513 12.33, SD = 3.76) had a positive effect on the four ecosystem functions, all other predictors of
514 each model being held statistically constant (Table 3). It was the predictor with the strongest
515 effect on the multifunctionality metric, with the second strongest effect on the NH_4^+ and NO_{2+3}
516 fluxes and with the smallest effect on the SOD (Fig. 6). Increasing the water temperature by
517 one population SD increases the different functions by 0.23 (SOD) to 0.52 (multifunctionality,
518 SD = 0.83) population SD (Table 3).



519
520
521
522

Figure 6. Partial linear regression plots (left) and standardized partial regression coefficients (effect sizes, right) of the predictors retained in the minimal adequate models explaining the

523 standardized ecosystem functions (sediment oxygen demand (SOD), ammonium flux (NH_4^+),
524 sum of nitrate and nitrite fluxes (NO_{2+3}) and the multifunctionality metric). Abundance (abund.)
525 and biomass (biom.) refer to the engineer *S. alveolata* abundance and biomass, respectively.
526 FDis_{ab} and FEve_{ab} refer to the functional dispersion and functional evenness, respectively, both
527 weighted by species abundance.

528

529 4. DISCUSSION

530 The study of the link between taxonomic diversity, functional diversity and ecosystem
531 functions is complex but crucial if we are to understand in a more holistic way ecosystem
532 functioning and the impact of disturbances on this functioning (Brose and Hillebrand, 2016;
533 Gamfeldt et al., 2015). Using *Sabellaria alveolata* reefs as a study case, we started to fill the
534 gap relative to the role played by biodiversity in the functions performed by tubicolous
535 structural engineers (Berke, 2010), building upon studies on the biogeochemical functioning of
536 bivalve reefs (see Stief (2013) and references therein). This study is a necessary first step
537 towards conceiving more controlled *in situ* experiments by removing potentially key species
538 such as highly mobile biodiffusors (*e.g. Eulalia viridis*) or manipulating the physical
539 disturbance of the reef by clearing out small *S. alveolata* tube patches.

540

541 4.1. Biogenic structures promote biogeochemical fluxes in coastal waters

542 Microorganisms and meiofauna were probably the main drivers of the oxygen and solute
543 fluxes measured in the soft sediments surrounding the engineered sediments along with
544 physico-chemical mechanisms such as diffusion and advection. Indeed, solutes transfer
545 mechanisms inside the first 10 cm of these soft sediments are probably dominated by advection
546 in the highly permeable CS sediments and by diffusion in the less permeable MS sediments
547 (Huettel et al., 2003). Macroinvertebrates were also relatively scarce with average abundances
548 between 226 ind.m⁻² (winter) and 4145 ind.m⁻² (spring) in the MS, 636 ind.m⁻² (winter) and

549 1556 ind.m⁻² (spring) in the CS. Consequently, macrofauna was probably not a driving force in
550 these sediments, either in terms of solute transfer via bioturbation or in terms of oxygen uptake
551 as indicated by a macrofauna-normalized SOD above 1 (Clough et al., 2005). Conversely,
552 macrofauna was across the three periods the main driver of the engineered sediment oxygen
553 uptake, as indicated by a macrofauna-normalized SOD close or below 1 (Clough et al., 2005).
554 Since, we did not measure microbial respiration or biomass during our study, we focused on
555 the engineered sediments for which we had information on what appeared to be the driving
556 force of its biogeochemical functioning, the macrofauna.

557 Across the three periods, we measured higher SOD, NH₄⁺ and NO₂₊₃ fluxes in the
558 engineered sediments compared to the CS and MS, a difference we attribute at least partly to
559 the 8 (summer) to 1000 (winter) times higher macrofauna biomass in the UES and DES
560 compared to the CS and MS. Indeed, community biomass and oxygen consumption are often
561 strongly correlated (Braeckman et al., 2010; Clough et al., 2005; Norkko et al., 2013) through
562 the positive link between individual body mass and respiration rate (Gillooly et al., 2001;
563 Hildrew et al., 2007). Macrofauna can also account for 10 to 70% of community NH₄⁺ fluxes
564 from the sediment through ammonium excretion (Kristensen, 1988; Vanni, 2002). Despite
565 representing between 45 and 97% of the macrofauna abundance in the engineered sediments,
566 *Sabellaria alveolata* creates, through the structures it builds and its biological activity, an
567 environment favorable to other macroinvertebrates (Dubois et al., 2002; Jones et al., 2018) and
568 probably also to a community of meiofauna and microorganisms (Ataide et al., 2014;
569 Kristensen and Kostka, 2005; Passarelli et al., 2014). Indeed, meiofauna and especially
570 nematodes are often more diverse and abundant inside biogenic structures such as *Sabellaria*
571 *wilsoni* reefs compared to neighboring bare sediments (Ataide et al., 2014). Furthermore, the
572 colonization of macrofauna tubes by prokaryotic communities is known to be stimulated by the
573 host's organic secretions that represent a food source for these organisms, probably affecting

574 global biogeochemical processes (Kristensen and Kostka, 2005; Passarelli et al., 2014). For
575 example, burrows built by polychaetes like *Hediste diversicolor*, that penetrate the anaerobic
576 subsurface sediment, promote microbial abundance and activity, increasing O₂ consumption
577 and nutrient release from the sediment (Mermillod-Blondin et al., 2004; Reise, 1981).
578 Consequently, meiofauna and even more so microorganisms surely play an important part in
579 the engineered sediments biogeochemical fluxes, mainly through aerobic respiration, dissolved
580 inorganic nitrogen excretion, particulate organic nitrogen remineralization, ammonium
581 assimilation, nitrification and denitrification (Herbert, 1999; Kristensen, 1988; Vanni, 2002).

582 Overall, oxygen consumption, ammonium and oxidized nitrogen release were enhanced in
583 the sediments engineered by *S. alveolata* compared to bare substratum, as reported for bivalve
584 reefs (Kellogg et al., 2013; Norling and Kautsky, 2007). The mechanisms promoting
585 biogeochemical fluxes in *S. alveolata* reefs and other polychaete reefs are probably the same as
586 in bivalve reefs and involve the dense macrofauna and the associated microorganisms
587 (Passarelli et al., 2014; Stief, 2013). First, the engineered structures (bivalve shells or
588 polychaete tubes) extend the surface available for colonization by nitrifying and denitrifying
589 microorganisms, which benefit from the metabolic waste products excreted by the engineer
590 species (ammonium and carbon dioxide). Second, microorganisms can use the large amounts
591 of biodeposits, including large quantities of extracellular polymeric substances such as mucus,
592 produced by bivalves and polychaetes (*i.e.* egestion of particulate organic matter), as a source
593 of labile organic matter (Gutiérrez et al., 2003; Heisterkamp et al., 2013).

594

595 4.2. *Biogeochemical fluxes in engineered habitats: a comparison*

596 We compared our results with fluxes measured in a polychaete reef built by the invasive
597 serpulid polychaete *Ficopomatus enigmaticus* (Keene, 1980), in a restored subtidal *Crassostrea*
598 *virginica* reef (Kellogg et al., 2013) and in a mudflat structured by *Upogedia pugettensis*, a

599 bioirrigating shrimp (D'Andrea and DeWitt, 2009) (Table 4). The two polychaete reefs had
600 close community respiration rates (between the spring DES values and the early March values)
601 and maximal NO_{2+3} fluxes (between the summer UES values and the November values) while
602 maximal NH_4^+ fluxes were two folds higher in our study (spring DES) compared with the
603 November values. For close water temperatures (12°C in this study and 14.5°C in Kellogg et
604 al. (2013)), the respiration rates measured in the *S. alveolata* and *C. virginica* reefs were close.
605 The maximal NH_4^+ and NO_{2+3} fluxes measured for the *S. alveolata* reef were comparable to the
606 ones measured respectively in April and June at the restored oyster reef. Finally, maximal daily
607 community respiration rates and NH_4^+ fluxes in this study were like the ones reported for the
608 high *U. pugettensis* density plots (Table 4). Differently, maximal NO_{2+3} fluxes measured in the
609 engineered sediments were two folds greater than the ones recorded in high *U. pugettensis*
610 density plots.

611 This comparison highlights a few interesting points on biogeochemical fluxes and
612 ecosystem engineers. First, the extend and the shape of the polychaete reefs seems to affect
613 NH_4^+ fluxes probably via the amount of organic matter trapped inside and between the
614 engineered structures. Indeed, *S. alveolata* reefs are composed of coalescent hummock
615 structures that completely recover the initial substrate (Jones et al., 2018) whereas *F.*
616 *enigmaticus* reefs are discontinuous structures between which water can pass and flush out the
617 accumulated organic matter (Bruschetti et al., 2011). Second, structural engineers like *S.*
618 *alveolata* and oysters that build coalescent structures, enhance in similar amounts sediment
619 oxygen demand, ammonium, and nitrates + nitrites fluxes. Finally, habitats built by reef-
620 forming species such as bivalve and tubicolous structural engineers could have a higher
621 potential as organic nitrogen recyclers than burrowing and bioturbating infauna like *U.*
622 *pugettensis* in engineered soft sediments (Berke, 2010).

623 **Table 4.** Sediment oxygen demand (SOD), ammonium (NH₄⁺) and nitrate + nitrite fluxes (NO₂₊₃) measured in engineered habitats built by
 624 polychaetes, bivalves and crustaceans and reported in this study and three others. D'Andrea & DeWitt (2009) measured fluxes in a mudflat
 625 colonized by low, medium, and high densities of *Upogedia pugettensis*.

Engineered habitat	Study location and reference	Type of flux reported	SOD	NH ₄ ⁺	NO ₂₊₃
<i>Sabellaria alveolata</i> (polychaete) reef	English Channel coast (bay of Mont-Saint-Michel, France), this study	Min – max across spring (12°C), summer (17°C) and winter (8°C)	0.03 (winter DES) – 0.33 (spring DES) g O ₂ .m ⁻² .h ⁻¹	0.06 (winter DES) – 0.85 (spring UES) mmol.m ⁻² .h ⁻¹	0.17 (winter DES) – 1.01 (summer UES) mmol.m ⁻² .h ⁻¹
		Min – max in spring and summer (daily values)	Spring: 8.03 (193) – 10.31 (247) Summer: 3.08 (74) – 4.24 (102) mmol O ₂ .m ⁻² .h ⁻¹	Spring: 0.65 (15.6) – 0.85 (20.4) Summer: 0.25 (6) – 0.70 (16.8) mmol.m ⁻² .h ⁻¹	Spring: 0.38 (9.12) – 0.53 (12.72) Summer: 0.32 (7.68) – 1.01 (24.24) mmol.m ⁻² .h ⁻¹
<i>Ficopomatus enigmaticus</i> (polychaete) reef	Mediterranean Sea (Tunisia), Keene 1980	exact temperature unknown	0.24 (early March) – 1.17 (late March) g O ₂ .m ⁻² .h ⁻¹	0.40 (November) mmol.m ⁻² .h ⁻¹	1.05 (November) mmol.m ⁻² .h ⁻¹
Restored <i>Crassostrea virginica</i> (bivalve) reef	Maryland coast (USA), Kellogg et al. 2013	Comparable values	12.87 mmol O ₂ .m ⁻² .h ⁻¹ (November, 14.5°C)	0.8 mmol.m ⁻² .h ⁻¹ (April, 15.1°C)	0.46 mmol.m ⁻² .h ⁻¹ 1.3 mmol.m ⁻² .h ⁻¹ (June, 25.7°C)
Mudflat colonized by bioirrigating shrimp <i>Upogedia pugettensis</i> (crustacean)	Oregon coast (USA), D'Andrea & DeWitt 2009	Summer (17.1°C)	97.4 (low density) – 225.7 (high density) mmol m ⁻² .d ⁻¹	7.11 (low density) – 16.37 (high density) mmol m ⁻² .d ⁻¹	1.16 (medium density) – 11.38 (high density) mmol m ⁻² .d ⁻¹

627 4.3. *Sabellaria alveolata* and water temperature are the main drivers of the engineered
628 sediment biogeochemical functioning

629 What we termed the engineer effect (*i.e.* the engineer *S. alveolata* promotes, through its
630 density, the biogeochemical functioning of the engineered sediments) mainly results from the
631 combined biological activity of the engineer species *S. alveolata per se*, as well as the
632 meiofauna and microorganisms associated to each individual and its tube, a community likely
633 specific to complex structures like polychaete tubes (Mermillod-Blondin et al., 2004; Reise,
634 1981; Tout et al., 2014) with a temperature-dependent activity (Herbert, 1999; Thamdrup et al.,
635 1998). This study based on observational data helped us to determine some of the main drivers
636 of the biogeochemical functioning of a *S. alveolata* reef; the engineer, the water temperature
637 and the associated macrofauna through their biological traits, strongly supporting the engineer
638 effect hypothesis and giving some support to the diversity hypothesis but only at relatively low
639 levels of functional diversity. The use of terms like “effect” or “driver” are somehow abusive
640 since real causality between predictors and response variables can only be determined through
641 controlled experiments. Nonetheless, we believe this study is a first step towards better
642 understanding the functioning of these complex habitats, helping us to better conserve and
643 manage them.

644 In sediments engineered by *S. alveolata*, the number one driver of community respiration,
645 was *S. alveolata* biomass. Water temperature was not the main driver of SOD like we expected
646 according to the Q10 of 2 relation (Hildrew et al., 2007) and subtidal studies on soft sediments
647 and oyster reefs (Janson et al., 2012; Kellogg et al., 2013). Nonetheless, temperature still had a
648 small positive effect on the SOD. We measured the highest SOD values in spring (12°C) and
649 not in summer (17°C), a difference we mainly attribute to the 2-3 times higher engineer biomass
650 in spring compared to summer, but also to the ripe and heavy individuals ready to spawn in
651 spring (Dubois et al., 2007a). Biomass can have a strong influence on respiration rates at the

652 individual and community level, a biomass effect we observed here which clearly surpassed the
653 effect of temperature on the SOD (Braeckman et al., 2010; Clough et al., 2005; Hildrew et al.,
654 2007; Norkko et al., 2013). Structural ecosystem engineers such as *S. alveolata* can also act as
655 agents of biogeochemical heterogeneity through the structural changes they cause, affecting
656 heat transfer processes and temperature dependent microbial activity (Gutiérrez et al., 2003).
657 Temperature loggers placed inside the reefs revealed that the engineered sediments present
658 lower heat transfers than the surrounding coarse sediments (Jones, pers. obs.), indicating water
659 temperature variations could be buffered inside these sediments, probably reducing
660 temperature-dependent aerobic respiration (Thamdrup et al., 1998; Woodin et al., 2010).

661 *Sabellaria alveolata* biomass was also the number one driver of the NH_4^+ fluxes, a result
662 probably caused by two processes positively correlated to the engineer biomass and stronger in
663 spring than in summer: excretion and egestion. First, the engineer biomass has a positive effect
664 on the NH_4^+ fluxes probably because of higher excretion rates of *S. alveolata* in spring when its
665 mean biomass is the highest, a seasonality also recorded for the gastropod *Crepidula fornicata*
666 (Martin et al., 2006). *Sabellaria alveolata* probably also egests more feces and pseudofeces
667 (Dubois et al., 2006) in spring during the phytoplankton bloom and the main reproductive
668 season, as recorded for *Modiolus modiolus* (Navarro and Thompson, 1997). These biodeposits
669 are rapidly remineralized by associated bacteria, producing NH_4^+ (Stief, 2013) and linking the
670 engineer biomass and NH_4^+ fluxes. Temperature was the second most important driver of the
671 NH_4^+ fluxes, an effect probably linked to the temperature-dependent metabolic rates of the meio
672 and macrofauna (excretion and egestion) and associated bacteria (nitrogen remineralization)
673 (Gillooly et al., 2001; Magni et al., 2000).

674 The first and second most important drivers of NO_{2+3} fluxes were *S. alveolata* abundance
675 and water temperature, respectively, probably through the promotion of nitrification by the
676 engineer and its tube and the temperature-dependent activity of nitrifying bacteria. The

677 transformation of NH_4^+ into NO_2^- and then NO_3^- requires ammonium, oxygen, and the presence
678 of aerobic nitrifying microorganisms, more active at higher water temperatures (Herbert, 1999).
679 First, a diverse community of microorganisms including nitrifying bacteria are probably
680 directly associated to the surface of *S. alveolata* as shown for other polychaetes, amphipods and
681 bivalve soft tissues (Welsh and Castadelli, 2004). Secondly, *S. alveolata* density is also an
682 indirect measure of tube density, tubes that are home to nitrifying bacteria (D'Andrea and
683 DeWitt, 2009) and act as vectors allowing oxygen to penetrate deeper into the engineered
684 sediment, ultimately promoting nitrification. Finally, the vertical movements of *S. alveolata* in
685 its tube increases the oxygen fluxes from the overlying water to the deeper engineered sediment
686 layers further promoting nitrification, as reported in the burrows of many soft sediment
687 organisms (Woodin et al., 2010).

688

689 4.4. *Biological traits of associated macrofauna is a secondary driver of the engineered* 690 *sediments biogeochemical functioning*

691 Using a multiple linear regression approach, we never detected a significant effect of indices
692 only used to test the diversity hypothesis (SR, N1 and FRic) or the mass-ratio hypothesis (FIde1
693 and FIde3), on a flux. If there is an effect of a higher associated macrofauna diversity or
694 biological trait dominance on the fluxes, it is mostly accounted for by *S. alveolata* abundance
695 or biomass (engineer effect hypothesis) and by functional dispersion (FDis) or functional
696 evenness (FEve) (diversity and mass ratio hypotheses). Indeed, a decrease in the abundance of
697 *S. alveolata* is linked to an opposite increase in the abundance and richness of associated
698 macrofauna (Dubois et al., 2002; Jones et al., 2018). Furthermore, 75% of the species richness
699 variability can be explained by *S. alveolata* biomass (negative effect) and FDis_{ab} (positive
700 effect). Finally, FDis_{ab} and FIde1_{ab} have a 0.99 correlation indicating FDis_{ab} increases with an

701 abundance increase of higher mobility species (movement capacity trait) and this index can also
702 be used to test the mass-ratio hypothesis.

703 Functional dispersion, only weighted by abundance, was the second most important driver
704 of the SOD and multifunctionality metric, displaying in both cases a concave form (second
705 degree polynomial form with a negative effect size), a form also detected in sandy sediments
706 when relating benthic species richness and ammonium fluxes (Thrush et al., 2017). Maximal
707 values of the two functions were detected for $FDis_{ab}$ values of *ca.* 0.19 for SOD and *ca.* 0.16
708 for the multifunctionality metric, corresponding to the middle of the disturbance continuum
709 present in the engineered sediments (slightly disturbed reefs). Bumped-shaped relationships
710 seem to be relatively common in cross community studies possibly because the explanatory
711 variables are more variable and have a wider range of values in these studies than in a single
712 community type helping to detect these functional forms (Mittelbach et al., 2001; Thrush and
713 Lohrer, 2012). We deliberately sampled two different engineered sediment typologies
714 characterized by different communities dominated by the engineer species but with a large
715 diversity gradient, favoring the detection of this concave functional form.

716 Mechanisms linked to the diversity hypothesis such as resource partitioning and niche
717 complementarity (Tilman, 1997) or non-additive interactions among species through trait
718 redundancy (insurance hypothesis, Yachi and Loreau (1999)) probably explain the positive
719 effect low functional diversity has on the SOD and the global biogeochemical functioning
720 (Brose and Hillebrand, 2016). The presence of species with modalities like *S. alveolata*,
721 especially regarding their mobility (*e.g.* *Magallana gigas*, *Mytilus cf. galloprovincialis*), limit
722 the functional loss due to the increasing disturbance and the resulting decrease of the engineer
723 species abundance (Dubois et al., 2006, 2002). Other species with no to low movement
724 capacities and with modalities complementary to *S. alveolata* (*e.g.* *Venerupis corrugata*)

725 regarding other traits (*e.g.* sediment reworking) enhance the global biogeochemical functioning
726 of the engineered sediments (Bruno et al., 2003; Stachowicz, 2001).

727 In a second phase, interferences between species' modalities (*i.e.* interference competition)
728 seem to limit biogeochemical processes like organic matter remineralization, leading to the
729 negative effect of high functional diversity on biogeochemical fluxes (Brose and Hillebrand,
730 2016). Indeed, structural engineers such as *S. alveolata* likely build habitats where the local
731 environmental conditions are optimal for them and where they are likely the best performing
732 species of the assemblage for most ecosystem functions, including biogeochemical fluxes
733 (Gamfeldt et al., 2015). Consequently, a functional dispersion above 0.16-0.19 could translate
734 into a stronger spatial and/or trophic competition between the associated macrofauna and *S.*
735 *alveolata* (Dubois et al., 2006; Jones et al., 2018), potentially leading to lower metabolic rates
736 of the engineer species (*e.g.* respiration) and to lower global fluxes. Functionally dissimilar
737 species could also disrupt the local conditions created by the engineer, for example through the
738 destruction of *S. alveolata* tubes (*e.g.* *Carcinus maenas* excavate *S. alveolata* tubes), decreasing
739 nutrient cycling.

740 Furthermore, functional dispersion weighted by abundance had a strictly negative effect on
741 the NH_4^+ fluxes. Considering the strong correlation between FDis_{ab} and FId_{ab} , this result
742 supports the mass-ratio hypothesis and is probably linked to the same mechanisms as the ones
743 explaining the negative effect of higher functional diversity levels on the SOD and
744 multifunctionality. Even at low functional diversity levels, we did not detect a positive effect
745 of increasing diversity on the NH_4^+ fluxes. The loss of *S. alveolata* type species in terms of
746 mobility and the addition of species with different modality combinations seems to rapidly
747 impair NH_4^+ fluxes, probably through the loss of sessile bivalves and polychaetes, organisms
748 that strongly influence these fluxes through excretion and biodeposit production (Stief, 2013).

749 Finally, functional evenness (abundance weighted only), an index informing on the
750 regularity of the abundance distribution in the functional space, had a weak negative effect on
751 the NO₂₊₃ fluxes. A high value of FEve indicates a homogenous distribution of the species and
752 of their abundance in the functional space with similar distance between species (Villéger et
753 al., 2008). Consequently, NO₂₊₃ fluxes seem to be promoted by the presence of several clumps
754 of species with similar trait combinations, indicating that a certain level of biological trait
755 redundancy associated to a certain level of species richness (*ca.* 10 species), is necessary for an
756 optimal nitrogen cycling in the reef.

757

758 4.5. *Global biogeochemical functioning of the engineered sediments*

759 Overall, the biogeochemical functioning of the sediments engineered by *S. alveolata* was
760 much more intense than that of the soft sediments surrounding the engineered sediments, a
761 difference likely linked to the abundant and diversified macrofauna, meiofauna and
762 microorganisms promoted by the reef structures and the engineer itself. Focusing on the
763 engineered sediments, we found that water temperature is the main driver of their global
764 biogeochemical functioning, followed by *S. alveolata* biomass and the macrofauna functional
765 dispersion weighted by abundance. Consequently, tubicolous structural engineers such as *S.*
766 *alveolata* have biomass-dependent effects on biogeochemical fluxes as do burrowing and
767 bioturbating infauna (Braeckman et al., 2010; D'Andrea and DeWitt, 2009; Norkko et al., 2013;
768 Thrush et al., 2017), suggesting this could be a general property of many marine ecosystem
769 engineers. Furthermore, the concave effect FDis_{ab} has on the multifunctionality metric brings
770 support to the diversity hypothesis at low levels of functional dispersion (0.01-0.16), when
771 sessile species with complementarity modalities for other traits dominate the engineered
772 sediments. When functional dispersion is higher (0.16-0.36), the biogeochemical functioning
773 of the engineered sediments is promoted by higher abundances of species with no to low

774 movement capacities (higher $F_{Ide1_{ab}}$), bringing support to the mass-ratio hypothesis, as found
775 in autotrophic terrestrial systems (Díaz et al., 2007; Garnier et al., 2004; Mokany et al., 2008)
776 and across field studies on soil fauna (Gagic et al., 2015). The concave effect of $F_{Dis_{ab}}$ on the
777 multifunctionality metric also indicates an intermediate macrofauna trait diversity could
778 maximize the global biogeochemical functioning of a *S. alveolata* reef through trait redundancy
779 and niche complementarity.

780 Maintaining a high abundance and biomass of the engineer species appears paramount if we
781 wish to further maintain ecosystem processes performed by this habitat such as organic matter
782 remineralization and nitrogen cycling; indeed, our results evidence that a good physical status
783 of the reef structure (prograding areas with high tube density) leads to a good ecological
784 functioning of the reef. Local disturbances (reef degradation) can increase species number
785 (Dubois et al., 2020) and possibly enhance functional diversity, which does not appear, at first,
786 as detrimental in terms of biogeochemical fluxes. However, anthropogenic disturbances such
787 as trampling should be limited as much as possible, as they could alter *S. alveolata* biomass in
788 the long term (Desroy et al., 2011; Plicanti et al., 2016). Complementary studies should aim at
789 manipulating disturbance levels and/or species composition, measuring other functions such as
790 primary and secondary production or consumption and studying other *S. alveolata* reefs to test
791 if engineer biomass and functional dispersion weighted by abundance could be used as
792 indicators of *S. alveolata* reef functioning.

793

794 **CONCLUSION**

795 In a conservation goal, identifying indices that inform us on the global functioning of
796 ecosystems and its evolution is paramount. In the case of *S. alveolata* reefs, our study indicates
797 the two most important parameters to measure are the biomass and abundance of the engineer
798 species. In a second step, estimating the abundance of the associated species (and not their

799 biomass) and focusing on their respective movement capacities, a trait associated to a species'
800 sediment reworking abilities (Queirós et al., 2013) and known to affect many biogeochemical
801 fluxes (Braeckman et al., 2010; Ieno et al., 2006; Mermillod-Blondin et al., 2005; Michaud et
802 al., 2005), can help to evaluate more precisely the reef's biogeochemical functioning. Biomass
803 is often considered as more functionally relevant than abundance especially when the process
804 is size-based (Gagic et al., 2015; Mouillot et al., 2011) and large macrofauna have been shown
805 to play a prominent role in soft sediment biogeochemical fluxes (Norkko et al., 2013; Thrush
806 et al., 2006). Nonetheless, soft sediments engineered into hard substrata by *S. alveolata* act as
807 an environmental filter and only relatively small organisms can establish between the engineer
808 tubes and affect biogeochemical fluxes (Jones et al., 2018). Consequently, in this highly size-
809 constrained habitat, abundance appears to be more important than biomass in explaining
810 biogeochemical fluxes.

811

812 **Acknowledgements**

813 This project was funded by an EC2CO DRIL (CNRS) grant. A. G. J. was supported by the
814 "Laboratoire d' Excellence" LabexMER (ANR-10-LABX-19) and co-funded by a grant from
815 the French government under the program "Investissements d'Avenir" and by a Région
816 Bretagne/Ifremer PhD grant. Our funding source was not involved in the different phases of
817 this study. We thank all the people that helped us on the field (Flavie Delanzy, Ludovic Goyot,
818 Bernard Delaunay) and in the lab (Angelica Navarro, Célia Bellengier, Louise Lanrivain).
819 Finally, we wish to thank the two anonymous reviewers who helped improve this manuscript.

820

821 **References**

822

823 Ataide, M.B., Venekey, V., Filho, J.S.R., Santos, P.J.P. dos, 2014. Sandy reefs of *Sabellaria*
824 *wilsoni* (Polychaeta: Sabellariidae) as ecosystem engineers for meiofauna in the
825 Amazon coastal region, Brazil. *Marine Biodiversity* 44, 403–413.
826 <https://doi.org/10.1007/s12526-014-0248-x>

- 827 Ayata, S.-D., Ellien, C., Dumas, F., Dubois, S., Thiebaut, E., 2009. Modelling larval dispersal
828 and settlement of the reef-building polychaete *Sabellaria alveolata*: Role of
829 hydroclimatic processes on the sustainability of biogenic reefs. *Continental Shelf*
830 *Research* 29, 1605–1623. <https://doi.org/10.1016/j.csr.2009.05.002>
- 831 Berke, S.K., 2010. Functional groups of ecosystem engineers: a proposed classification with
832 comments on current issues. *Integr. Comp. Biol.* 50, 147–157.
833 <https://doi.org/10.1093/icb/icq077>
- 834 Bonnot-Courtois, C., Fournier, J., Dréau, A., 2004. Recent morphodynamics of shell banks in
835 the western part of the Bay of Mont-Saint-Michel (France) / Morphodynamique actuelle
836 des bancs coquilliers dans la partie occidentale de la baie du Mont-Saint-Michel
837 (France). *Géomorphologie: relief, processus, environnement* 10, 65–79.
838 <https://doi.org/10.3406/morfo.2004.1200>
- 839 Bouma, T.J., Olenin, S., Reise, K., Ysebaert, T., 2009. Ecosystem engineering and biodiversity
840 in coastal sediments: posing hypotheses. *Helgoland Marine Research* 63, 95–106.
841 <https://doi.org/10.1007/s10152-009-0146-y>
- 842 Braeckman, U., Provoost, P., Gribsholt, B., Van Gansbeke, D., Middelburg, J.J., Soetaert, K.,
843 Vincx, M., Vanaverbeke, J., 2010. Role of macrofauna functional traits and density in
844 biogeochemical fluxes and bioturbation. *Marine Ecology Progress Series* 399, 173–186.
845 <https://doi.org/10.3354/meps08336>
- 846 Brose, U., Hillebrand, H., 2016. Biodiversity and ecosystem functioning in dynamic
847 landscapes. *Philos. Trans. R. Soc. Lond., B, Biol. Sci.* 371.
848 <https://doi.org/10.1098/rstb.2015.0267>
- 849 Bruno, J.F., Stachowicz, J.J., Bertness, M.D., 2003. Incorporating facilitation into ecological
850 theory. *Trends in Ecology and Evolution* 18, 119–125. [https://doi.org/10.1016/S0169-5347\(02\)00045-9](https://doi.org/10.1016/S0169-5347(02)00045-9)
- 851
- 852 Bruschetti, M., Bazterrica, C., Fanjul, E., Luppi, T., Iribarne, O., 2011. Effect of biodeposition
853 of an invasive polychaete on organic matter content and productivity of the sediment in
854 a coastal lagoon. *Journal of Sea Research* 66, 20–28.
855 <https://doi.org/10.1016/j.seares.2011.04.007>
- 856 Cadotte, M.W., 2017. Functional traits explain ecosystem function through opposing
857 mechanisms. *Ecol Lett* 20, 989–996. <https://doi.org/10.1111/ele.12796>
- 858 Cardinale, B.J., Matulich, K.L., Hooper, D.U., Byrnes, J.E., Duffy, E., Gamfeldt, L., Balvanera,
859 P., O'Connor, M.I., Gonzalez, A., 2011. The functional role of producer diversity in
860 ecosystems. *American journal of botany* 98, 572–592. <https://doi.org/10.1111/j.1461-0248.2007.01037.x>
- 861
- 862 Chevenet, F., Dolédec, S., Chessel, D., 1994. A fuzzy coding approach for the analysis of long-
863 term ecological data. *Freshwater Biology* 31, 295–309. <https://doi.org/10.1111/j.1365-2427.1994.tb01742.x>
- 864
- 865 Clough, L.M., Renaud, P.E., Ambrose Jr., W.G., 2005. Impacts of water depth, sediment
866 pigment concentration, and benthic macrofaunal biomass on sediment oxygen demand
867 in the western Arctic Ocean. *Can. J. Fish. Aquat. Sci.* 62, 1756–1765.
868 <https://doi.org/10.1139/f05-102>
- 869 Covich, A.P., Austen, M.C., Bärlocher, F., Chauvet, E., Cardinale, B.J., Biles, C.L., Inchausti,
870 P., Dangles, O., Solan, M., Gessner, M.O., 2004. The role of biodiversity in the
871 functioning of freshwater and marine benthic ecosystems. *BioScience* 54, 767–775.
- 872 Curd, A., Pernet, F., Corporeau, C., Delisle, L., Firth, L.B., Nunes, F.L.D., Dubois, S.F., 2019.
873 Connecting organic to mineral: How the physiological state of an ecosystem-engineer
874 is linked to its habitat structure. *Ecological Indicators* 98, 49–60.
875 <https://doi.org/10.1016/j.ecolind.2018.10.044>

- 876 D'Andrea, A.F., DeWitt, T.H., 2009. Geochemical ecosystem engineering by the mud shrimp
877 *Upogebia pugettensis* (Crustacea: Thalassinidae) in Yaquina Bay, Oregon: Density-
878 dependent effects on organic matter remineralization and nutrient cycling. *Limnol.*
879 *Oceanogr.* 54, 1911–1932. <https://doi.org/10.4319/lo.2009.54.6.1911>
- 880 Desroy, N., Dubois, S.F., Fournier, J., Ricquiers, L., Le Mao, P., Guerin, L., Gerla, D.,
881 Rougerie, M., Legendre, A., 2011. The conservation status of *Sabellaria alveolata* (L.)
882 (Polychaeta: Sabellariidae) reefs in the Bay of Mont-Saint-Michel. *Aquatic*
883 *Conservation: Marine and Freshwater Ecosystems* 21, 462–471.
884 <https://doi.org/10.1002/aqc.1206>
- 885 Dias, A.S., Paula, J., 2001. Associated fauna of *Sabellaria alveolata* colonies on the central
886 coast of Portugal. *Journal of the Marine Biological Association of the United Kingdom*
887 81, 169–170. <https://doi.org/10.1017/S0025315401003538>
- 888 Díaz, S., Lavorel, S., Bello, F. de, Quétier, F., Grigulis, K., Robson, T.M., 2007. Incorporating
889 plant functional diversity effects in ecosystem service assessments. *PNAS* 104, 20684–
890 20689. <https://doi.org/10.1073/pnas.0704716104>
- 891 Dubois, S., Commito, J.A., Olivier, F., Retière, C., 2006. Effects of epibionts on *Sabellaria*
892 *alveolata* (L.) biogenic reefs and their associated fauna in the Bay of Mont Saint-Michel.
893 *Estuarine, Coastal and Shelf Science* 68, 635–646.
894 <https://doi.org/10.1016/j.ecss.2006.03.010>
- 895 Dubois, S., Comtet, T., Retière, C., Thiébaud, E., 2007a. Distribution and retention of *Sabellaria*
896 *alveolata* larvae (Polychaeta: Sabellariidae) in the Bay of Mont-Saint-Michel, France.
897 *Marine Ecology Progress Series* 346, 243–254. <https://doi.org/10.3354/meps07011>
- 898 Dubois, S., Orvain, F., MarinLal, J.C., Ropert, M., Lefebvre, S., 2007b. Small-scale spatial
899 variability of food partitioning between cultivated oysters and associated suspension-
900 feeding species, as revealed by stable isotopes. *Marine Ecology Progress Series* 336,
901 151–160. <https://doi.org/10.3354/meps336151>
- 902 Dubois, S., Retière, C., Olivier, F., 2002. Biodiversity associated with *Sabellaria alveolata*
903 (Polychaeta: Sabellariidae) reefs: effects of human disturbances. *Journal of the Marine*
904 *Biological Association of the United Kingdom* 82, 817–826.
905 <https://doi.org/10.1017/S0025315402006185>
- 906 ETI BioInformatics, n.d. Marine species identification portal [WWW Document]. *Marine*
907 *Species Identification Portal*. URL <http://species-identification.org/index.php>
- 908 Fauchald, K., Jumars, P.A., 1979. *The diet of worms: a study of polychaete feeding guilds*.
909 Aberdeen University Press.
- 910 Gagic, V., Bartomeus, I., Jonsson, T., Taylor, A., Winqvist, C., Fischer, C., Slade, E.M.,
911 Steffan-Dewenter, I., Emmerson, M., Potts, S.G., Tschardt, T., Weisser, W.,
912 Bommarco, R., 2015. Functional identity and diversity of animals predict ecosystem
913 functioning better than species-based indices. *Proceedings of the Royal Society B:*
914 *Biological Sciences* 282, 20142620. <https://doi.org/10.1098/rspb.2014.2620>
- 915 Gamfeldt, L., Lefcheck, J.S., Byrnes, J.E.K., Cardinale, B.J., Duffy, J.E., Griffin, J.N., 2015.
916 Marine biodiversity and ecosystem functioning: what's known and what's next? *Oikos*
917 124, 252–265. <https://doi.org/10.1111/oik.01549>
- 918 Garnier, E., Cortez, J., Billès, G., Navas, M.-L., Roumet, C., Debussche, M., Laurent, G.,
919 Blanchard, A., Aubry, D., Bellmann, A., Neill, C., Toussaint, J.-P., 2004. Plant
920 functional markers capture ecosystem properties during secondary succession. *Ecology*
921 85, 2630–2637. <https://doi.org/10.1890/03-0799>
- 922 Gillooly, J.F., Brown, J.H., West, G.B., Savage, V.M., Charnov, E.L., 2001. Effects of size and
923 temperature on metabolic rate. *Science* 293, 2248–2251.
924 <https://doi.org/10.1126/science.1061967>

- 925 Godbold, J.A., Bulling, M.T., Solan, M., 2011. Habitat structure mediates biodiversity effects
 926 on ecosystem properties. *Proceedings of the Royal Society of London B: Biological*
 927 *Sciences* 278, 2510–2518. <https://doi.org/10.1098/rspb.2010.2414>
- 928 Godbold, J.A., Solan, M., 2009. Relative importance of biodiversity and the abiotic
 929 environment in mediating an ecosystem process. *Marine Ecology Progress Series* 396,
 930 273–282. <https://doi.org/10.3354/meps08401>
- 931 Goldberg, W.M., 2013. *The biology of reefs and reef organisms*. The University of Chicago
 932 Press, Chicago and London.
- 933 Gray, J.S., 2000. The measurement of marine species diversity, with an application to the
 934 benthic fauna of the Norwegian continental shelf. *Journal of Experimental Marine*
 935 *Biology and Ecology* 250, 23–49. [https://doi.org/10.1016/S0022-0981\(00\)00178-7](https://doi.org/10.1016/S0022-0981(00)00178-7)
- 936 Grime, J.P., 1998. Benefits of plant diversity to ecosystems: immediate, filter and founder
 937 effects. *Journal of Ecology* 86, 902–910. <https://doi.org/10.1046/j.1365-2745.1998.00306.x>
- 939 Gruet, Y., 1986. Spatio-temporal changes of sabellarian reefs built by the sedentary polychaete
 940 *Sabellaria alveolata* (Linne). *Marine Ecology* 7, 303–319.
 941 <https://doi.org/10.1111/j.1439-0485.1986.tb00166.x>
- 942 Gruet, Y., 1972. Aspects morphologiques et dynamiques de constructions de l'Annelide
 943 polychete *Sabellaria alveolata* (Linne). *Revue des Travaux de l'Institut des Pêches*
 944 *Maritimes* 36, 131–161.
- 945 Guerra-García, J.M., Tierno de Figueroa, J.M., Navarro-Barranco, C., Ros, M., Sánchez-
 946 Moyano, J.E., Moreira, J., 2014. Dietary analysis of the marine Amphipoda (Crustacea:
 947 Peracarida) from the Iberian Peninsula. *Journal of Sea Research* 85, 508–517.
 948 <https://doi.org/10.1016/j.seares.2013.08.006>
- 949 Gutiérrez, J.L., Jones, C.G., 2006. Physical ecosystem engineers as agents of biogeochemical
 950 heterogeneity. *BioScience* 56, 227–236. [https://doi.org/10.1641/0006-3568\(2006\)056\[0227:PEEAAO\]2.0.CO;2](https://doi.org/10.1641/0006-3568(2006)056[0227:PEEAAO]2.0.CO;2)
- 952 Gutiérrez, J.L., Jones, C.G., Strayer, D.L., Iribarne, O.O., 2003. Mollusks as ecosystem
 953 engineers: the role of shell production in aquatic habitats. *Oikos* 101, 79–90.
 954 <https://doi.org/10.1034/j.1600-0706.2003.12322.x>
- 955 Hector, A., Schmid, B., Beierkuhnlein, C., Caldeira, M.C., Diemer, M., Dimitrakopoulos, P.G.,
 956 Finn, J.A., Freitas, H., Giller, P.S., Good, J., Harris, R., Högberg, P., Huss-Danell, K.,
 957 Joshi, J., Jumpponen, A., Körner, C., Leadley, P.W., Loreau, M., Minns, A., Mulder,
 958 C.P.H., O'Donovan, G., Otway, S.J., Pereira, J.S., Prinz, A., Read, D.J., Scherer-
 959 Lorenzen, M., Schulze, E.-D., Siamantziouras, A.-S.D., Spehn, E.M., Terry, A.C.,
 960 Troumbis, A.Y., Woodward, F.I., Yachi, S., Lawton, J.H., 1999. Plant diversity and
 961 productivity experiments in european grasslands. *Science* 286, 1123–1127.
 962 <https://doi.org/10.1126/science.286.5442.1123>
- 963 Heisterkamp, I.M., Schramm, A., Larsen, L.H., Svenningsen, N.B., Lavik, G., de Beer, D.,
 964 Stief, P., 2013. Shell biofilm-associated nitrous oxide production in marine molluscs:
 965 processes, precursors and relative importance. *Environmental Microbiology* 15, 1943–
 966 1955. <https://doi.org/10.1111/j.1462-2920.2012.02823.x>
- 967 Herbert, R.A., 1999. Nitrogen cycling in coastal marine ecosystems. *FEMS Microbiol Rev* 23,
 968 563–590. <https://doi.org/10.1111/j.1574-6976.1999.tb00414.x>
- 969 Hewitt, J.E., Thrush, S.F., Halliday, J., Duffy, C., 2005. The importance of small-scale habitat
 970 structure for maintaining beta diversity. *Ecology* 86, 1619–1626.
 971 <https://doi.org/10.1890/04-1099>
- 972 Hildrew, A.G., Raffaelli, D.G., Edmonds-Brown, R., 2007. *Body size: the structure and*
 973 *function of aquatic ecosystems*. Cambridge University Press.
 974 <https://doi.org/10.1017/CBO9780511611223>

- 975 Hill, M.O., 1973. Diversity and evenness: a unifying notation and its consequences. *Ecology*
976 54, 427–432. <https://doi.org/10.2307/1934352>
- 977 Holt, T.J., Rees, E.I., Hawkins, S.J., Seed, R., 1998. Biogenic reefs. An overview of dynamic
978 and sensitivity characteristics for conservation management of marine SACs. Scottish
979 Association for Marine Science, UK Marine SACs Project.
- 980 Hooper, D.U., Chapin, F.S., Ewel, J.J., Hector, A., Inchausti, P., Lavorel, S., Lawton, J.H.,
981 Lodge, D.M., Loreau, M., Naeem, S., Schmid, B., Setälä, H., Symstad, A.J.,
982 Vandermeer, J., Wardle, D.A., 2005. Effects of biodiversity on ecosystem functioning:
983 a consensus of current knowledge. *Ecological Monographs* 75, 3–35.
984 <https://doi.org/10.1890/04-0922>
- 985 Hooper, D.U., Vitousek, P.M., 1997. The effects of plant composition and diversity on
986 ecosystem processes. *Science* 277, 1302–1305.
987 <https://doi.org/10.1126/science.277.5330.1302>
- 988 Huettel, M., Røy, H., Precht, E., Ehrenhauss, S., 2003. Hydrodynamical impact on
989 biogeochemical processes in aquatic sediments. *Hydrobiologia* 494, 231–236.
990 <https://doi.org/10.1023/A:1025426601773>
- 991 Ieno, E.N., Solan, M., Batty, P., Pierce, G.J., 2006. How biodiversity affects ecosystem
992 functioning: roles of infaunal species richness, identity and density in the marine
993 benthos. *Mar Ecol Prog Ser* 311, 263–271. <https://doi.org/10.3354/meps311263>
- 994 Intergovernmental Science-Policy Platform on Biodiversity and Ecosystem Services, I., 2019.
995 Summary for policymakers of the global assessment report on biodiversity and
996 ecosystem services of the Intergovernmental Science-Policy Platform on Biodiversity
997 and Ecosystem Services. Zenodo. <https://doi.org/10.5281/zenodo.3553579>
- 998 Janson, A.L., Denis, L., Rauch, M., Desroy, N., 2012. Macrobenthic biodiversity and oxygen
999 uptake in estuarine systems: The example of the Seine estuary. *Journal of Soils and*
1000 *Sediments* 12, 1568–1580. <https://doi.org/10.1007/s11368-012-0557-2>
- 1001 Jones, A.G., Dubois, S.F., Desroy, N., Fournier, J., 2018. Interplay between abiotic factors and
1002 species assemblages mediated by the ecosystem engineer *Sabellaria alveolata*
1003 (Annelida: Polychaeta). *Estuarine, Coastal and Shelf Science*.
1004 <https://doi.org/10.1016/j.ecss.2017.10.001>
- 1005 Jones, C.G., Lawton, J.H., Shachak, M., 1997. Positive and negative effects of organisms as
1006 physical ecosystem engineers. *Ecology* 78, 1946–1957. [https://doi.org/10.1890/0012-9658\(1997\)078\[1946:PANEEO\]2.0.CO;2](https://doi.org/10.1890/0012-9658(1997)078[1946:PANEEO]2.0.CO;2)
- 1008 Jones, C.G., Lawton, J.H., Shachak, M., 1994. Organisms as ecosystem engineers. *Oikos* 69,
1009 373–386. <https://doi.org/10.2307/3545850>
- 1010 Jones, J.G., Berner, R.A., Meadows, P.S., Durand, B., Eglinton, G., Eglinton, G., Curtis, C.D.,
1011 McKenzie, D.P., Murchison, D.G., 1985. Microbes and microbial processes in
1012 sediments. *Philosophical Transactions of the Royal Society of London. Series A,*
1013 *Mathematical and Physical Sciences* 315, 3–17. <https://doi.org/10.1098/rsta.1985.0025>
- 1014 Jumars, P.A., Dorgan, K.M., Lindsay, S.M., 2015. Diet of worms emended: an update of
1015 polychaete feeding guilds. *Annual Review of Marine Science* 7, 497–520.
1016 <https://doi.org/10.1146/annurev-marine-010814-020007>
- 1017 Keene, W.C., 1980. The importance of a reef-forming polychaete, *Mercierella enigmatica*
1018 fauvel, in the oxygen and nutrient dynamics of a hypereutrophic subtropical lagoon.
1019 *Estuarine and Coastal Marine Science* 11, 167–178. [https://doi.org/10.1016/S0302-3524\(80\)80039-9](https://doi.org/10.1016/S0302-3524(80)80039-9)
- 1021 Kellogg, M.L., Cornwell, J.C., Owens, M.S., Paynter, K.T., 2013. Denitrification and nutrient
1022 assimilation on a restored oyster reef. *Marine Ecology Progress Series* 480, 1–19.
1023 <https://doi.org/10.3354/meps10331>

- 1024 Kristensen, E., 2008. Mangrove crabs as ecosystem engineers; with emphasis on sediment
1025 processes. *Journal of sea Research* 59, 30–43.
1026 <https://doi.org/10.1016/j.seares.2007.05.004>
- 1027 Kristensen, E., 1988. Benthic fauna and biogeochemical processes in marine sediments:
1028 microbial activities and fluxes, in: *Nitrogen Cycling in Coastal Marine Environments*.
1029 Blackburn, T.H., Sørensen, J., Chichester, pp. 275–299.
- 1030 Kristensen, E., Kostka, J.E., 2005. Macrofaunal burrows and irrigation in marine sediment:
1031 microbiological and biogeochemical interactions, in: *Interactions between Macro- and*
1032 *Microorganisms in Marine Sediments, Coastal and Estuarine Studies*. American
1033 Geophysical Union (AGU), pp. 125–157. <https://doi.org/10.1029/CE060p0125>
- 1034 Laliberté, E., Legendre, P., 2010. A distance-based framework for measuring functional
1035 diversity from multiple traits. *Ecology* 91, 299–305. <https://doi.org/10.1890/08-2244.1>
- 1036 Lavorel, S., Garnier, E., 2002. Predicting changes in community composition and ecosystem
1037 functioning from plant traits: revisiting the Holy Grail. *Functional Ecology* 16, 545–
1038 556. <https://doi.org/10.1046/j.1365-2435.2002.00664.x>
- 1039 Le Cam, J.-B., Fournier, J., Etienne, S., Couden, J., 2011. The strength of biogenic sand reefs:
1040 Visco-elastic behaviour of cement secreted by the tube building polychaete *Sabellaria*
1041 *alveolata*, Linnaeus, 1767. *Estuarine, Coastal and Shelf Science* 91, 333–339.
1042 <https://doi.org/10.1016/j.ecss.2010.10.036>
- 1043 Lejart, M., Clavier, J., Chauvaud, L., Hily, C., 2012. Respiration and calcification of
1044 *Crassostrea gigas*: contribution of an intertidal invasive species to coastal ecosystem
1045 co2 fluxes. *Estuaries and Coasts* 35, 622–632. <https://doi.org/10.1007/s12237-011-9462-y>
- 1047 Magni, P., Montani, S., Takada, C., Tsutsumi, H., 2000. Temporal scaling and relevance of
1048 bivalve nutrient excretion on a tidal flat of the Seto Inland Sea, Japan. *Marine Ecology*
1049 *Progress Series* 198, 139–155. <https://doi.org/10.3354/meps198139>
- 1050 MarLIN, 2006. BIOTIC [WWW Document]. BIOTIC - Biological Traits Information
1051 Catalogue. URL www.marlin.ac.uk/biotic
- 1052 Martin, S., Thouzeau, G., Chauvaud, L., Jean, F., Guérin, L., Clavier, J., 2006. Respiration,
1053 calcification, and excretion of the invasive slipper limpet, *Crepidula fornicata* L.:
1054 Implications for carbon, carbonate, and nitrogen fluxes in affected areas. *Limnol.*
1055 *Oceanogr.* 51, 1996–2007. <https://doi.org/10.4319/lo.2006.51.5.1996>
- 1056 Mermillod-Blondin, F., François-Carcaillet, F., Rosenberg, R., 2005. Biodiversity of benthic
1057 invertebrates and organic matter processing in shallow marine sediments: an
1058 experimental study. *Journal of Experimental Marine Biology and Ecology* 315, 187–
1059 209. <https://doi.org/10.1016/j.jembe.2004.09.013>
- 1060 Mermillod-Blondin, F., Rosenberg, R., François-Carcaillet, F., Norling, K., Mauclaire, L.,
1061 2004. Influence of bioturbation by three benthic infaunal species on microbial
1062 communities and biogeochemical processes in marine sediment. *Aquatic Microbial*
1063 *Ecology* 36, 271–284. <https://doi.org/10.3354/ame036271>
- 1064 Michaud, E., Desrosiers, G., Mermillod-Blondin, F., Sundby, B., Stora, G., 2005. The
1065 functional group approach to bioturbation: The effects of biodiffusers and gallery-
1066 diffusers of the *Macoma balthica* community on sediment oxygen uptake. *Journal of*
1067 *Experimental Marine Biology and Ecology* 326, 77–88.
1068 <https://doi.org/10.1016/j.jembe.2005.05.016>
- 1069 Mittelbach, G.G., Steiner, C.F., Scheiner, S.M., Gross, K.L., Reynolds, H.L., Waide, R.B.,
1070 Willig, M.R., Dodson, S.I., Gough, L., 2001. What is the observed relationship between
1071 species richness and productivity? *Ecology* 82, 2381–2396.
1072 [https://doi.org/10.1890/0012-9658\(2001\)082\[2381:WITORB\]2.0.CO;2](https://doi.org/10.1890/0012-9658(2001)082[2381:WITORB]2.0.CO;2)

- 1073 Mokany, K., Ash, J., Roxburgh, S., 2008. Functional identity is more important than diversity
1074 in influencing ecosystem processes in a temperate native grassland. *Journal of Ecology*
1075 96, 884–893. <https://doi.org/10.1111/j.1365-2745.2008.01395.x>
- 1076 Mouillot, D., Graham, N.A.J., Villéger, S., Mason, N.W.H., Bellwood, D.R., 2013. A functional
1077 approach reveals community responses to disturbances. *Trends in Ecology & Evolution*
1078 28, 167–177. <https://doi.org/10.1016/j.tree.2012.10.004>
- 1079 Mouillot, D., Villéger, S., Scherer-Lorenzen, M., Mason, N.W., 2011. Functional structure of
1080 biological communities predicts ecosystem multifunctionality. *PLoS one* 6, e17476.
1081 <https://doi.org/10.1371/journal.pone.0017476>
- 1082 Muir, A.P., Nunes, F.L.D., Dubois, S.F., Pernet, F., 2016. Lipid remodelling in the reef-building
1083 honeycomb worm, *Sabellaria alveolata*, reflects acclimation and local adaptation to
1084 temperature. *Scientific Reports* 6. <https://doi.org/10.1038/srep35669>
- 1085 Naeem, S., Håkansson, K., Lawton, J.H., Crawley, M.J., Thompson, L.J., 1996. Biodiversity
1086 and plant productivity in a model assemblage of plant species. *Oikos* 76, 259–264.
1087 <https://doi.org/10.2307/3546198>
- 1088 Navarro, J.M., Thompson, R.J., 1997. Biodeposition by the horse mussel *Modiolus modiolus*
1089 (*Dillwyn*) during the spring diatom bloom. *Journal of Experimental Marine Biology and*
1090 *Ecology* 209, 1–13. [https://doi.org/10.1016/0022-0981\(96\)02681-0](https://doi.org/10.1016/0022-0981(96)02681-0)
- 1091 Navarro-Barranco, C., Tierno-de-Figueroa, J.M., Guerra-García, J.M., Sánchez-Tocino, L.,
1092 García-Gómez, J.C., 2013. Feeding habits of amphipods (Crustacea: Malacostraca)
1093 from shallow soft bottom communities: comparison between marine caves and open
1094 habitats. *Journal of Sea Research* 78, 1–7. <https://doi.org/10.1016/j.seares.2012.12.011>
- 1095 Newell, R.I.E., Cornwell, J.C., Owens, M.S., 2002. Influence of simulated bivalve
1096 biodeposition and microphytobenthos on sediment nitrogen dynamics: A laboratory
1097 study. *Limnol. Oceanogr.* 47, 1367–1379. <https://doi.org/10.4319/lo.2002.47.5.1367>
- 1098 Noernberg, M.A., Fournier, J., Dubois, S., Populus, J., 2010. Using airborne laser altimetry to
1099 estimate *Sabellaria alveolata* (Polychaeta: Sabellariidae) reefs volume in tidal flat
1100 environments. *Estuarine, Coastal and Shelf Science* 90, 93–102.
1101 <https://doi.org/10.1016/j.ecss.2010.07.014>
- 1102 Norkko, A., Villnäs, A., Norkko, J., Valanko, S., Pilditch, C., 2013. Size matters: implications
1103 of the loss of large individuals for ecosystem function. *Sci Rep* 3, 1–7.
1104 <https://doi.org/10.1038/srep02646>
- 1105 Norling, P., Kautsky, N., 2007. Structural and functional effects of *Mytilus edulis* on diversity
1106 of associated species and ecosystem functioning. *Marine Ecology Progress Series* 351,
1107 163–175. <https://doi.org/10.3354/meps07033>
- 1108 Passarelli, C., Olivier, F., Paterson, D.M., Meziane, T., Hubas, C., 2014. Organisms as
1109 cooperative ecosystem engineers in intertidal flats. *Journal of Sea Research* 92, 92–101.
1110 <https://doi.org/10.1016/j.seares.2013.07.010>
- 1111 Plicanti, A., Domínguez, R., Dubois, S.F., Bertocci, I., 2016. Human impacts on biogenic
1112 habitats: Effects of experimental trampling on *Sabellaria alveolata* (Linnaeus, 1767)
1113 reefs. *Journal of Experimental Marine Biology and Ecology* 478, 34–44.
1114 <https://doi.org/10.1016/j.jembe.2016.02.001>
- 1115 Porta, B.L., Nicoletti, L., 2009. *Sabellaria alveolata* (Linnaeus) reefs in the central Tyrrhenian
1116 Sea (Italy) and associated polychaete fauna. *Zoosymposia* 2, 527–536.
1117 <https://doi.org/10.11646/zoosymposia.2.1.36>
- 1118 Queirós, A.M., Birchenough, S.N.R., Bremner, J., Godbold, J.A., Parker, R.E., Romero-
1119 Ramirez, A., Reiss, H., Solan, M., Somerfield, P.J., Van Colen, C., Van Hoey, G.,
1120 Widdicombe, S., 2013. A bioturbation classification of European marine infaunal
1121 invertebrates. *Ecol Evol* 3, 3958–3985. <https://doi.org/10.1002/ece3.769>

- 1122 Reise, K., 1981. High abundance of small zoobenthos around biogenic structures in tidal
1123 sediments of the Wadden Sea. *Helgolander Meeresunters* 34, 413–425.
1124 <https://doi.org/10.1007/BF01995914>
- 1125 Revsbech, N.P., 1989. An oxygen microsensor with a guard cathode. *Limnol. Oceanogr.* 34,
1126 474–478. <https://doi.org/10.4319/lo.1989.34.2.0474>
- 1127 Romero, G.Q., Gonçalves-Souza, T., Vieira, C., Koricheva, J., 2015. Ecosystem engineering
1128 effects on species diversity across ecosystems: a meta-analysis. *Biological Reviews* 90,
1129 877–890. <https://doi.org/10.1111/brv.12138>
- 1130 Schielzeth, H., 2010. Simple means to improve the interpretability of regression coefficients.
1131 *Methods in Ecology and Evolution* 1, 103–113. [https://doi.org/10.1111/j.2041-
1132 210X.2010.00012.x](https://doi.org/10.1111/j.2041-210X.2010.00012.x)
- 1133 Shumway, S.E., 1979. The effects of body size, oxygen tension and mode of life on the oxygen
1134 uptake rates of polychaetes. *Comparative Biochemistry and Physiology Part A: Physiology* 64,
1135 273–278. [https://doi.org/10.1016/0300-9629\(79\)90660-1](https://doi.org/10.1016/0300-9629(79)90660-1)
- 1136 Smyth, A.R., Geraldi, N.R., Thompson, S.P., Piehler, M.F., 2016. Biological activity exceeds
1137 biogenic structure in influencing sediment nitrogen cycling in experimental oyster reefs.
1138 *Marine Ecology Progress Series* 560, 173–183. <https://doi.org/10.3354/meps11922>
- 1139 Solan, M., Cardinale, B.J., Downing, A.L., Engelhardt, K.A.M., Ruesink, J.L., Srivastava, D.S.,
1140 2004. Extinction and ecosystem function in the marine benthos. *Science* 306, 1177–
1141 1180. <https://doi.org/10.1126/science.1103960>
- 1142 Stachowicz, J.J., 2001. Mutualism, facilitation, and the structure of ecological communities
1143 positive interactions play a critical, but underappreciated, role in ecological
1144 communities by reducing physical or biotic stresses in existing habitats and by creating
1145 new habitats on which many species depend. *BioScience* 51, 235–246.
1146 [https://doi.org/10.1641/0006-3568\(2001\)051\[0235:MFATSO\]2.0.CO;2](https://doi.org/10.1641/0006-3568(2001)051[0235:MFATSO]2.0.CO;2)
- 1147 Stief, P., 2013. Stimulation of microbial nitrogen cycling in aquatic ecosystems by benthic
1148 macrofauna: mechanisms and environmental implications. *Biogeosciences* 10, 7829–
1149 7846. <https://doi.org/10.5194/bg-10-7829-2013>
- 1150 Thamdrup, B., Hansen, J.W., Jørgensen, B.B., 1998. Temperature dependence of aerobic
1151 respiration in a coastal sediment. *FEMS Microbiol Ecol* 25, 189–200.
1152 <https://doi.org/10.1111/j.1574-6941.1998.tb00472.x>
- 1153 Thrush, S.F., Hewitt, J.E., Gibbs, M., Lundquist, C., Norkko, A., 2006. Functional role of large
1154 organisms in intertidal communities: community effects and ecosystem function.
1155 *Ecosystems* 9, 1029–1040. <https://doi.org/10.1007/s10021-005-0068-8>
- 1156 Thrush, S.F., Hewitt, J.E., Kraan, C., Lohrer, A.M., Pilditch, C.A., Douglas, E., 2017. Changes
1157 in the location of biodiversity–ecosystem function hot spots across the seafloor
1158 landscape with increasing sediment nutrient loading. *Proc. R. Soc. B* 284, 20162861.
1159 <https://doi.org/10.1098/rspb.2016.2861>
- 1160 Thrush, S.F., Lohrer, A.M., 2012. Why bother going outside: the role of observational studies
1161 in understanding biodiversity-ecosystem function relationships, in: *Marine Biodiversity
1162 and Ecosystem Functioning: Frameworks, Methodologies, and Integration*. Oxford
1163 University Press.
- 1164 Tilman, D., 1997. Community invasibility, recruitment limitation, and grassland biodiversity.
1165 *Ecology* 78, 81–92. [https://doi.org/10.1890/0012-
1166 9658\(1997\)078\[0081:CIRLAG\]2.0.CO;2](https://doi.org/10.1890/0012-9658(1997)078[0081:CIRLAG]2.0.CO;2)
- 1167 Tout, J., Jeffries, T.C., Webster, N.S., Stocker, R., Ralph, P.J., Seymour, J.R., 2014. Variability
1168 in microbial community composition and function between different niches within a
1169 coral reef. *Microb Ecol* 67, 540–552. <https://doi.org/10.1007/s00248-013-0362-5>

- 1170 Tréguer, P., Le Corre, P., 1975. Manuel d'analyse des sels nutritifs dans l'eau de mer,
1171 Laboratoire d'Océanographie Chimique. Université de Bretagne Occidentale, Brest,
1172 France.
- 1173 Vanni, M.J., 2002. Nutrient cycling by animals in freshwater ecosystems. *Annual Review of*
1174 *Ecology and Systematics* 33, 341–370.
1175 <https://doi.org/10.1146/annurev.ecolsys.33.010802.150519>
- 1176 Villéger, S., Mason, N.W.H., Mouillot, D., 2008. New multidimensional functional diversity
1177 indices for a multifaceted framework in functional ecology. *Ecology* 89, 2290–2301.
1178 <https://doi.org/10.1890/07-1206.1>
- 1179 Welsh, D.T., Castadelli, G., 2004. Bacterial nitrification activity directly associated with
1180 isolated benthic marine animals. *Marine Biology* 144, 1029–1037.
1181 <https://doi.org/10.1007/s00227-003-1252-z>
- 1182 Woodin, S.A., Wethey, D.S., Volkenborn, N., 2010. Infaunal hydraulic ecosystem engineers:
1183 cast of characters and impacts. *Integrative and Comparative Biology* 50, 176–187.
- 1184 Yachi, S., Loreau, M., 1999. Biodiversity and ecosystem productivity in a fluctuating
1185 environment: The insurance hypothesis. *Proc Natl Acad Sci U S A* 96, 1463–1468.
- 1186 Zuur, A.F., Ieno, E.N., Elphick, C.S., 2010. A protocol for data exploration to avoid common
1187 statistical problems. *Methods in Ecology and Evolution* 1, 3–14.
1188 <https://doi.org/10.1111/j.2041-210X.2009.00001.x>
1189

1 **Supplementary material**

2 **Table S1.** Mean (n = 12) abundance and biomass (ash-free dry weight in mg) of all the species
 3 identified in the undisturbed and disturbed engineered sediments. The mean was calculated over
 4 the three seasons and the four cores sampled for each engineered sediment type.

Species name	Abbreviated name	Undisturbed engineered sediment		Disturbed engineered sediment	
		Density (ind .m ⁻²)	Biomass (AFDW mg.m ⁻²)	Density (ind .m ⁻²)	Biomass (AFDW mg.m ⁻²)
<i>Achelia</i> sp.	ACHsp	38	4	599	61
<i>Axelsonia littoralis</i>	ALIT	0	0	47	0
<i>Amphipholis squamata</i>	ASQU	9	5	156	32
<i>Corophium arenarium</i>	CARE	0	0	5	0
<i>Carcinus maenas</i>	CMAE	71	858	61	631
<i>Corophium</i> sp.	CORsp	33	5	207	34
<i>Cereus pedunculatus</i>	CPED	439	67	104	846
<i>Cirriformia tentaculata</i>	CTEN	5	1	28	8
<i>Eulalia ornata</i>	EORN	170	65	0	0
<i>Eumida sanguinea</i>	ESAN	24	17	24	38
<i>Eulalia viridis</i>	EVIR	71	168	52	517
<i>Gnathia maxilaris</i>	GMAX	0	0	5	20
<i>Golfingia vulgaris</i>	GVUL	85	813	156	1 369
<i>Lekanesphaera</i> sp.	LEKsp	179	313	269	541
<i>Lumbrinereis</i> sp.	LUMsp	0	0	5	1
<i>Magallana gigas</i>	MGIG	0	0	9	4 347
<i>Mytilus</i> cf. <i>galloprovincialis</i>	McfGAL	47	89	132	251
<i>Mediomastus fragilis</i>	MFRA	24	1	85	15
<i>Molgula</i> sp.	MOLsp	14	80	5	32
<i>Melita palmata</i>	MPAL	28	5	137	47
<i>Mysta picta</i>	MPIC	0	0	10	2
<i>Nematoda</i> spp.	NEMA	726	185	1 151	103
<i>Nemertean</i>	NEME	231	1 637	278	1 311
<i>Nephtys</i> sp.	NEPsp	0	0	5	2
<i>Nephasoma minutum</i>	NMIN	250	71	189	47

<i>Odontosyllis ctenostoma</i>	OCTE	0	0	118	28
<i>Odontosyllis</i> sp.	ODOsp	42	9	42	5
<i>Polydora ciliata</i>	PCIL	9	9	0	0
<i>Perinereis cultrifera</i>	PCUL	47	207	141	209
<i>Pygospio elegans</i>	PELE	0	0	28	12
<i>Photys</i> sp.	PHOsp	24	0	0	0
<i>Pholoe inornata</i>	PINO	0	0	9	6
<i>Phyllodoce laminosa</i>	PLAM	0	0	38	269
<i>Polycirrus</i> sp.	POLYCsp	5	1	38	8
<i>Polydora</i> sp.	POLYDsp	5	1	0	0
<i>Porcellana platycheles</i>	PPLA	236	3 916	2 415	35 303
<i>Ruditapes philippinarum</i>	RPHI	0	0	9	325
<i>Sabellaria alveolata</i>	SALV	25 734	151 178	7 036	99 177
<i>Sphaerosyllis bulbosa</i>	SBUL	0	0	9	1
<i>Styela clava</i>	SCLA	0	0	19	130
<i>Syllis gracilis</i>	SGRA	5	4	14	4
<i>Spirobranchus lamarcki</i>	SLAM	5	11	52	76
<i>Venerupis corrugata</i>	VCOR	14	30	52	3 004
Total macrofauna including <i>S. alveolata</i>		28 532	159 746	13 140	148 751
Total macrofauna excluding <i>S. alveolata</i>		2 798	8 568	6 104	49 574
<i>S. alveolata</i> dominance (%)		90.19	94.64	53.55	66.67

6 **Table S2.** Mean (\pm SD, n = 4) sediment oxygen demand (SOD), ammonium fluxes (NH_4^+) and the sum of nitrate and nitrite fluxes (NO_{2+3})
7 measured during the spring, summer and winter campaigns for the four different sediment types, coarse sediments (CS), muddy sediments (MS),
8 undisturbed engineered sediments (UES) and disturbed engineered sediments (DES).

	Spring				Summer				Winter			
	CS	MS	UES	DES	CS	MS	UES	DES	CS	MS	UES	DES
SOD	414.7 \pm	1445.4 \pm	8032.65 \pm	10308.9 \pm	181.1 \pm	693.8 \pm	4294.6 \pm	3083.8 \pm	105.2 \pm	178.5 \pm	1276.0 \pm	843.8 \pm
($\mu\text{mol.m}^{-2}.\text{h}^{-1}$)	60.2	238.5	2426.51	1939.1	45.6	144.0	1259.2	718.8	33.3	62.9	166.9	429.3
NH_4^+	-0.8 \pm	-2.4 \pm	850.40 \pm	653.9 \pm	-4.4 \pm	42.4 \pm	698.2 \pm	249.7 \pm	-7.9 \pm	32.8 \pm	252.7 \pm	65.2 \pm
($\mu\text{mol.m}^{-2}.\text{h}^{-1}$)	1.0	0.6	121.79	269.0	1.2	67.2	359.2	49.1	1.3	8.8	62.1	31.0
NO_{2+3}	26.0 \pm	-43.7 \pm	381.87 \pm	534.2 \pm	35.6 \pm	0.2 \pm	1006.9 \pm	322.8 \pm	114.2 \pm	42.8 \pm	284.9 \pm	170.6 \pm
($\mu\text{mol.m}^{-2}.\text{h}^{-1}$)	13.4	20.3	108.61	166.2	8.8	0.7	463.8	89.0	51.3	17.3	14.2	64.3

Figure S3. Relation between the functional dispersion weighted by macrofauna abundance ($FDi_{s_{ab}}$) and the functional identity 1 weighted by macrofauna abundance ($FId_{e1_{ab}}$) considering the 24 engineered sediment cores. An increase of the $FId_{e1_{ab}}$ index is associated to an increase in the relative abundance of species with medium to high movement capacities.

